Available online at www.sciencedirect.com

ScienceDirect

Geochimica et Cosmochimica Acta 235 (2018) 463–482

Geochimica et Cosmochimica Acta

www.elsevier.com/locate/gca

Ground-truthing the planktic foraminifer-bound nitrogen isotope paleo-proxy in the Sargasso Sea

Sandi M. Smart [a,*], Haojia Ren [b], Sarah E. Fawcett [c], Ralf Schiebel [d], Maureen Conte [e], Patrick A. Rafter [f], Karen K. Ellis [g], Mira A. Weigand [g], Sergey Oleynik [g], Gerald H. Haug [d], Daniel M. Sigman [g]

[a] Department of Earth Sciences, Stellenbosch University, Private Bag X1, Matieland 7602, South Africa
[b] Department of Geosciences, National Taiwan University, Taipei 106, Taiwan
[c] Department of Oceanography, University of Cape Town, Rondebosch 7700, South Africa
[d] Climate Geochemistry Department, Max Planck Institute for Chemistry, 55128 Mainz, Germany
[e] Bermuda Institute of Ocean Sciences, St.George's GE 01, Bermuda
[f] Department of Earth System Science, University of California, Irvine, CA 92697, USA
[g] Department of Geosciences, Princeton University, Princeton, NJ 08544, USA

Received 8 December 2017; accepted in revised form 24 May 2018; available online 31 May 2018

Abstract

We report the nitrogen (N) isotope ratios ($\delta^{15}N$) of planktic foraminifera collected from upper-ocean net tows (surface to 200 m), moored sediment traps, and core-top sediments at the Bermuda Time-series Site in the northern Sargasso Sea between 2009 and 2013. Consistent with previous measurements from low-latitude core-top sediments, the annually-averaged $\delta^{15}N$ of organic matter bound within the shells of euphotic zone-dwelling, dinoflagellate symbiont-bearing foraminifera collected in net tows (2.3‰ on average) approximates that of shallow thermocline (~200 m) nitrate (2.6‰), the dominant source of new N to Sargasso Sea surface waters. Deeper-dwelling foraminifer species without dinoflagellate symbionts tend to have a higher $\delta^{15}N$ (3.6‰ on average). We observe no systematic difference between the bulk tissue and shell-bound $\delta^{15}N$ in net tow-collected foraminifera. A decline in shell N content is observed from net tows (6.8 nmol/mg) to sediment traps (5.4 nmol/mg) and surface sediment (3.0 nmol/mg). On average, shell-bound $\delta^{15}N$ rises from net tows (3.1‰) to sediment traps (3.7‰) but does not change further upon incorporation into the sediments (3.7‰). Together, these observations are consistent with preferential loss of shells or shell portions with lower $\delta^{15}N$ and higher N content during sinking through the upper 500 m, followed by a non-isotope fractionating decrease in N content between sinking and burial. Time-series data from sediment traps (and to a lesser extent, surface net tows) exhibit seasonal $\delta^{15}N$ variations, with a minimum in early spring, a maximum in late spring and a decline from summer to fall. These variations appear to arise from seasonal changes in the $\delta^{15}N$ of total upper-ocean biomass, which are, in turn, driven by early springtime nitrate supply, subsequent nitrate drawdown, and an increase in the relative importance of ammonium recycling into the late summer and early fall. The $\delta^{15}N$ connection between total upper ocean biomass and foraminifera indicates that foraminifer-bound $\delta^{15}N$ records the $\delta^{15}N$ of the annual nitrate supply in oligotrophic (e.g., subtropical) environments but will also be sensitive to the degree of nitrate consumption in high-nutrient regions and possibly to changes in upper-ocean ammonium recycling under some conditions.

Keywords: Planktic foraminifera; Nitrogen isotopes; Paleo-proxy

* Corresponding author.
E-mail address: sandi.smart@alumni.uct.ac.za (S.M. Smart).

https://doi.org/10.1016/j.gca.2018.05.023
0016-7037/

1. INTRODUCTION

The accumulation of organic matter on the seafloor archives information about past ocean productivity and nutrient conditions, key factors controlling the influence of biology on atmospheric carbon dioxide concentrations and thus global climate. Organic nitrogen (N) in marine sediments and sedimentary microfossils is a promising recorder of the N isotopic composition of nitrate (NO_3^-) supplied to phytoplankton in oligotrophic environments such as the subtropical gyres, which is in turn affected by and thus bears witness to processes such as N fixation and denitrification (Altabet and Curry, 1989). In addition, the N isotopes are a potential recorder of surface water nitrate consumption in nitrate-replete environments such as the Southern Ocean (François et al., 1992; Altabet and François, 1994).

When nitrate is consumed by phytoplankton, the lighter ^{14}N isotope is preferentially incorporated, causing the remaining nitrate pool (and thus also the particulate organic N (PON) subsequently produced from it) to become progressively enriched in the heavier ^{15}N isotope (i.e., increasing in $\delta^{15}N$, where $\delta^{15}N = \{[(^{15}N/^{14}N)_{sample}/(^{15}N/^{14}N)_{N2\ in\ air}] - 1\} \times 1000$; in units of per mil, ‰) (Wada and Hattori, 1978; Pennock et al., 1996; Waser et al., 1998; Sigman et al., 1999a). Thus, PON sinking to the seafloor carries with it the isotopic imprint of partial nitrate consumption in overlying waters. If the surface ocean nitrate pool is completely consumed, the $\delta^{15}N$ of the total accumulated PON converges on that of the initial nitrate supply. Thus, in oligotrophic environments where nitrate consumption in surface waters is always essentially complete, the $\delta^{15}N$ of sinking PON (and thus of N in underlying sediments) would be expected to match the $\delta^{15}N$ of the nitrate supply (Altabet, 1988; Altabet and François, 1994). Diagenetic alteration and/or exogenous N inputs, however, demonstrably influence the $\delta^{15}N$ of bulk sedimentary N (Altabet and François, 1994; Meckler et al., 2011) and have prompted a shift to analysis of N pools that are robust against these effects, with our focus here on microfossil-bound organic N (Sigman et al., 1999b; Robinson et al., 2004; Ren et al., 2009). With recent method developments, it is now feasible to analyze the N isotopes of the small amounts of organic N encased within the shells or 'tests' of planktic foraminifera (Ren et al., 2009; Ren et al., 2012; Straub et al., 2013), calcifying zooplankton that ubiquitously accumulate in deep-sea sediments.

Planktic foraminifera inhabit a wide range of ocean environments from the tropics to the poles and have a diversity of feeding habits. Shallow-dwelling species prey on zooplankton and larger phytoplankton, while deeper-dwelling species are sustained by detrital particles and/or the organisms that feed upon them (Bé et al., 1977; Spindler et al., 1984; Schiebel and Hemleben, 2017). Many shallower species also host algal symbionts: dinoflagellates in the case of most spinose, shallow-dwellers (Bé et al., 1977; Schiebel and Hemleben, 2017; and references therein), and other algae including chrysophytes in the case of some thermocline-dwellers (Gastrich, 1987; Faber et al., 1988). Foraminifera grow in size by adding chambers to their shells, using an organic sheet as a template for calcification (King and Hare, 1972; Bé et al., 1979; Spero, 1988). In this way, N-rich biomineralizing proteins are added prior to each chamber addition and are sequestered within the calcite matrix (Bé et al., 1977; Hemleben et al., 1989). Additional calcification during life (ontogenic) and reproduction (gametogenic) may further protect shell-associated organic matter, while post-mortem encrustation might protect both shell-native and external organic matter. In the tropical and subtropical open ocean, there is a strong link between the $\delta^{15}N$ of thermocline nitrate, the main source of nitrate to the euphotic zone (i.e., the well-lit layer from the surface to the 1% light level) (Altabet, 1988; Knapp et al., 2005), and the shell-bound $\delta^{15}N$ of most planktic foraminifer species in underlying surface sediments (Ren et al., 2009; Ren et al., 2012), supporting the utility of the planktic foraminifer-bound $\delta^{15}N$ proxy. However, important questions remain regarding the controls on foraminifer-bound $\delta^{15}N$. First, how does shell-bound $\delta^{15}N$ compare to the $\delta^{15}N$ of foraminiferal tissue, and is this relationship stable? Second, are there other factors besides the $\delta^{15}N$ of the annual nitrate supply to the euphotic zone that affect foraminifer-bound $\delta^{15}N$, and are these adequately important to cause significant changes through time? Third, is the $\delta^{15}N$ signal acquired in the upper ocean preserved as tests sink to the seafloor? If shell-bound $\delta^{15}N$ is altered, is the magnitude of this alteration constant and/or systematic? To address these unknowns, we present modern foraminiferal tissue and shell-bound $\delta^{15}N$ measurements for a range of species collected from the upper ocean, sediment traps, and surface sediments at the Bermuda Time-series Site in the Sargasso Sea.

The Bermuda region has a well-characterised seasonal cycle of mixing and primary production (Steinberg et al., 2001; Lomas et al., 2013). The deepest mixing occurs in late winter/early spring (down to 200–250 m), injecting thermocline nitrate into surface waters. As the surface ocean warms and the mixed layer shoals in the late spring and early summer, nitrate is drawn down rapidly by phytoplankton to less than 0.1 μM (Lipschultz, 2001), and its concentration generally remains extremely low throughout the summer and early fall stratification period (<0.01 μM) (Fawcett et al., 2015). A gradual deepening of the mixed layer occurs in late fall and winter as the surface ocean cools and wind-driven mixing erodes the strong thermal gradient. Even during the period of deepest mixing, however, nitrate concentrations typically remain well below 0.5 μM in the upper 100 m, or ~15% of the concentration present at 200–250 m (Fig. 1). Therefore, nitrate consumption in this region is close to complete almost year-round (Lipschultz, 2001; Fawcett et al., 2015) and the $\delta^{15}N$ of PON sinking out of the euphotic zone should equal the $\delta^{15}N$ of the original subsurface nitrate supply (Altabet, 1988; François et al., 1992). This balance is only weakly affected by the export of dissolved organic N and suspended particles (Knapp et al., 2005). Thus, by focusing our ground-truthing efforts on the oligotrophic ocean, we have sought to initially minimize the complication of partial nitrate consumption. The Bermuda Time-series Site is typical of the oligotrophic, subtropical open ocean gyres

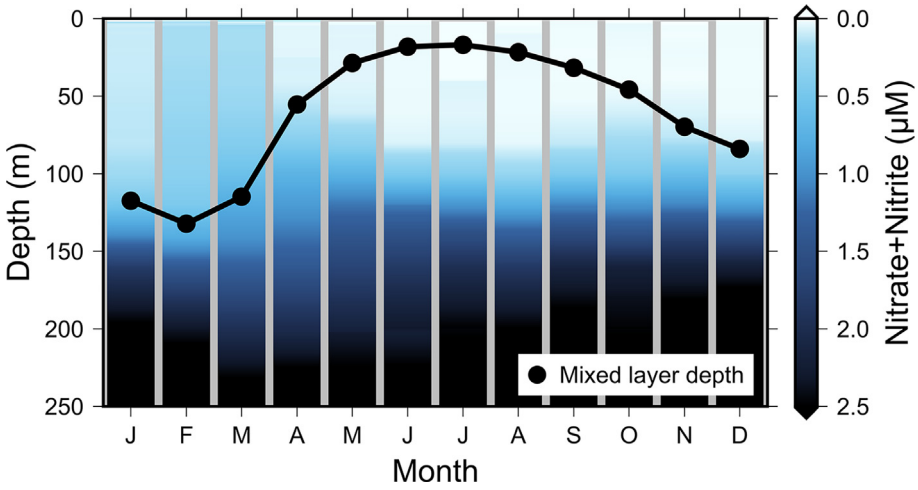

Fig. 1. Climatological average of upper-ocean (0–250 m) nitrate + nitrite concentration (in μM; color shading) and mixed layer depth (in meters; black circles) at the Bermuda Atlantic Time-series Study (BATS) site in the Sargasso Sea. Long-term monthly averages were computed using all BATS cruise data collected between October 1988 and December 2014 (available online at http://batsftp.bios.edu/BATS/). Mixed-layer depth is defined as the minimum depth at which potential temperature had decreased by ≥0.2 °C from a reference depth of 10 m (de Boyer Montégut et al., 2004). (For interpretation of the references to colour in this figure legend, the reader is referred to the web version of this article.)

(Steinberg et al., 2001; Lomas et al., 2013), making our findings broadly applicable to a large area of the global ocean.

In this ground-truthing study, we compare the $\delta^{15}N$ of living foraminifera caught in surface net tows, sinking shells collected in moored sediment traps and fossil shells present in core-top sediments. Together, these data capture foraminifer-bound N at important stages in its production and preservation, from incorporation of N into the living organism through diagenesis during sinking and burial in the sediments.

2. METHODS

2.1. Sample collection

Living foraminifera were collected from the upper water column using a 1-m^2, 200-μm-mesh plankton net during ten cruises between July 2011 and November 2013. Each tow lasted 2–3 h at a target depth between 0 m and 200 m (see Table A1 for details). Approximately 90% of the foraminifer-containing tow material was preserved in a 5–10% *p*H-buffered formalin solution and stored at 4 °C until processing (Ren et al., 2012). The remaining 10% was size-fractionated, filtered and freeze-dried for elemental and isotopic analysis of PON. Hydrographic data for each station were acquired from a Sea-Bird conductivity-temperature-depth (CTD) sensor mounted on a Niskin bottle rosette (data available online at http://batsftp.bios.edu/BATS/). Mixed layer depth was defined as the depth at which temperature had decreased by ≥0.2 °C from a reference depth of 10 m (de Boyer Montégut et al., 2004). Seawater samples collected from the Niskin bottles on the same cruises were measured for the concentration and N isotope ratios of nitrate and nitrate + nitrite (Fawcett et al., 2011, 2014, 2015). Foraminifer tests were picked from Oceanic Flux Program (OFP) sediment traps at 500 m, 1500 m and 3200 m water depth (Conte et al., 2001; Conte and Weber, 2014). The OFP mooring was located at 31°50′N, 64°10′W between November 2009 and November 2010, with each sample representing a two-week collection. To attain sufficient N for shell-bound analysis, specimens from two or all three trap depths were combined when needed. Core-top sediments were collected using a modified Van Veen corer at a nearby site (31°44′N, 64°05′W; 4570 m water depth – shallower than the lysocline; Honjo and Erez (1978)). Fossil foraminifer tests were picked from the >125 μm size fraction of the 0.5–2.0 cm depth interval. Carbon-14 dating of surface sediments from the vicinity (two cores at 31°45′N, 64°21′W; 4300 ± 100 m water depth; Haidar et al., 2000) suggests an average age of approximately one thousand years for our sediment samples; downcore foraminifer-bound $\delta^{15}N$ from the Caribbean indicates no change in the region during the late Holocene (Ren et al., 2009).

2.2. N isotope methods for foraminifer tissue, shells and particulate organic N

Foraminifera were isolated from bulk tow collections by density separation (addition of a 300 g/L NaCl solution), decanted into a watch glass and left in a fume hood until the formalin-seawater solution had evaporated. Between one and 100 individuals of the same species were picked per sample (depending on species availability and estimated N content) under a dissecting microscope using a wet picking brush. Picked samples were transferred to 5 mL Eppendorf tubes, rinsed several times with deionised water, briefly sonicated to loosen any detritus, and transferred to 12 mL pre-combusted Wheaton vials (Ren et al., 2012). After

pipetting off the supernatant liquid, samples were oven-dried at 30–40 °C. Dried specimens were gently crushed open with an ethanol-cleaned spatula, sonicated in deionised water and the external organic N (i.e., tissue) converted to nitrate by the persulfate oxidation method (Nydahl, 1978; Knapp et al., 2005) (see below).

After removal of the tissue N fraction, the remaining crushed shells were rinsed at least five times with deionised water and oven dried at 50 °C. Approximately 1–3 mg of cleaned calcite was weighed out into 4 mL pre-combusted Wheaton vials, combining samples of the same species (from different tows and occasionally different cruises, but always the same season) where necessary. The crushed tests were dissolved in 6 N hydrochloric acid (HCl) to release calcite-bound organic N into solution, and oxidised to nitrate by adding 1 mL of a basic persulfate oxidising reagent (POR; a potassium persulfate/sodium hydroxide solution) to each vial and autoclaving for 65 min on a slow vent setting (Nydahl, 1978; Knapp et al., 2005). Blanks (containing 4 mL POR) and three amino acid reference materials (AG, USGS-40 and USGS-41) were included in every batch of samples to ensure complete oxidation and correct for the N blank associated with the POR. USGS-40 and USGS-41 are international reference materials (both glutamic acid; Qi et al., 2003), and AG is an in-house mixed amino acid standard that has been calibrated by analysis of the mixed powder with elemental analyzer-isotope ratio mass spectrometry.

All resulting nitrate samples (from tissue and shell-bound N oxidations) were adjusted to a *p*H of 5–7 using HCl and measured for nitrate concentration by chemiluminescence (Braman and Hendrix, 1989). Finally, nitrate was converted to nitrous oxide using the bacterial conversion technique known as the "denitrifier method" (Sigman et al., 2001; Casciotti et al., 2002), followed by $\delta^{15}N$ measurement by gas chromatography–isotope ratio mass spectrometry using a Thermo MAT 253 with purpose-built online N_2O extraction and purification system (Sigman et al., 2001; Casciotti et al., 2002; Weigand et al., 2016). All $\delta^{15}N$ measurements were referenced to atmospheric N_2 using solutions of nitrate reference materials IAEA-NO3 and USGS-34, and oxidised samples were then corrected for the POR blank using the amino acid reference materials.

Foraminifera from sediment traps were analyzed for shell-bound $\delta^{15}N$ in the same way as the tow specimens. For the core-top shells, two additional cleaning steps were undertaken (after crushing) following Ren et al. (2015): (1) 5 min ultrasonication in 2% sodium hexametaphosphate (*p*H 8), and (2) reductive cleaning using sodium bicarbonate-buffered dithionite-citrate reagent. Replicate analyses were made when possible. For tow-caught foraminifera, pooled standard deviations (1σ) of tissue $\delta^{15}N$ and shell-bound $\delta^{15}N$ cleaning-and-oxidation replicates were 0.53‰ and 0.47‰, respectively. The relatively large standard deviation for shell-bound $\delta^{15}N$ may be partly due to higher (and more variable) blank/total N ratios (averaging 10%). However, this cannot explain the tissue standard deviations, as the blank contributes only ~4% on average. Rather, the fact that fewer individuals are combined to make a $\delta^{15}N$ measurement (typically 1–20 for tissue *vs.* hundreds for shells) is a likely contributor. The limited availability of shell specimens in core-top and sediment trap collections prevented replicate oxidations, but blanks only contributed 3–4% on average of the total sample N.

The $\delta^{15}N$ of size-fractionated PON (ranging from 200 μm to >5000 μm) collected in the upper 200 m during the net tows was determined by elemental analyzer-isotope ratio mass spectrometry (an Elementar Vario Isotope Cube online to an Elementar Isoprime visION), referencing to atmospheric N_2 using USGS-40 and an in-house aminocaproic acid standard. The pooled standard deviation of replicate measurements was 0.07‰. The $\delta^{15}N$ of sinking PON was analyzed on the <125 μm size fraction of sediment trap samples by mass spectrometry using either a Europa 20–20 or GV Isoprime mass spectrometer. Samples were acidified prior to analysis to remove carbonates using a modification of the Verrado et al. (1990) method.

2.3. Averaging foraminifer $\delta^{15}N$ and N content

Foraminifer $\delta^{15}N$ and N content averages (e.g., for each type of collection) were calculated using three different methods: first, the arithmetic (unweighted) average, where all species are assigned equal weight; second, the "$N_{measured}$-weighted" average, where each species is weighted by its contribution to the total amount of foraminifera N picked and measured; and third, the "$N_{present}$-weighted" average, where each species is weighted by its estimated contribution to the total amount of foraminiferal N (>100 μm) actually present in that environment. On the one hand, the second method does not account for the actual abundance of each species in the environment (i.e., it assumes that the picked specimens represent the species proportions in the original collection). On the other hand, the third method relies on estimations of the shell weights of each species and of species abundances from other studies.

For the net tows, contributions to $N_{present}$ were estimated from the mean annual species compositions of Tolderlund and Bé (1971) (from 0 to 10 m and 0–500 m plankton tows at Bermuda Station S) together with the average shell weights of Movellan (2013) (from 0 to 200 m tows in the North Atlantic, Caribbean, Arabian Sea and Red Sea) and Takahashi and Bé (1984) (from near-surface tows in the North Atlantic and Caribbean). For the sediment traps, N contributions were estimated from the annual test fluxes measured in the 1500 m OFP sediment trap during 2009–2010 (the same period as our trap-caught foraminifera) (Salmon et al., 2015) together with our own measurements of N per shell. For the core-top sediments, the contribution of each species was estimated from foraminifera counts at a nearby core site (V007067; 34° 40′N, 61°27′W; 4308 m water depth; CLIMAP Project Members, 1981, 1994) and average shell weights from North Atlantic and Caribbean deep-sea sediments (Takahashi and Bé, 1984). In the two cases where core-top shell-weight data were unavailable (*G. truncatulinoides* and *G. conglobatus*), weights were approximated using the average shell-weight of all the other species.

In the results section below, the $\delta^{15}N$ averages from all three calculation methods are presented: unweighted, $N_{measured}$-weighted, and $N_{present}$-weighted. However, given the focus of this study on N transfer and turnover and based on our assessment of uncertainties, we refer only to the $N_{measured}$-weighted average in the following discussion.

3. RESULTS

3.1. Overview of foraminifer $\delta^{15}N$ and N content

The $\delta^{15}N$ of foraminiferal tissue collected from net tows ranges from 1.5‰ to 4.7‰, while foraminifer shells from the same tows have a $\delta^{15}N$ ranging from 1.8‰ to 7.8‰. We note that the large size of the error bars for some species derives mainly from $\delta^{15}N$ variability between cruises (pooled cruise standard deviation of 1.09‰ for tissue, 1.33‰ for shell), which is larger than the variability between tows on the same cruise (pooled tow standard deviation of 0.82‰ for tissue, unavailable for shell) and, in turn, larger than the variability between measurements within a tow (pooled measurement standard deviation of 0.57‰ for tissue, 0.59‰ for shell; Table A2). The unweighted averages of all the tow data (light grey triangles in Fig. 2a) indicate a higher $\delta^{15}N$ for shells (3.6‰; n = 72) than for tissue (2.9‰; n = 452). Weighting the $\delta^{15}N$ of each species by its N contribution yields tissue and shell-bound $\delta^{15}N$ averages that are more similar to each other; 3.2‰ *vs.* 3.1‰, respectively, using $N_{measured}$ (black triangles) and 3.2‰ *vs.* 3.0‰, $\delta^{15}N$ respectively, using $N_{present}$ (dark grey triangles). The $\delta^{15}N$ of sinking shells (n = 86) ranges from 2.6‰ to 5.3‰ with an unweighted average of 4.0‰, and weighted

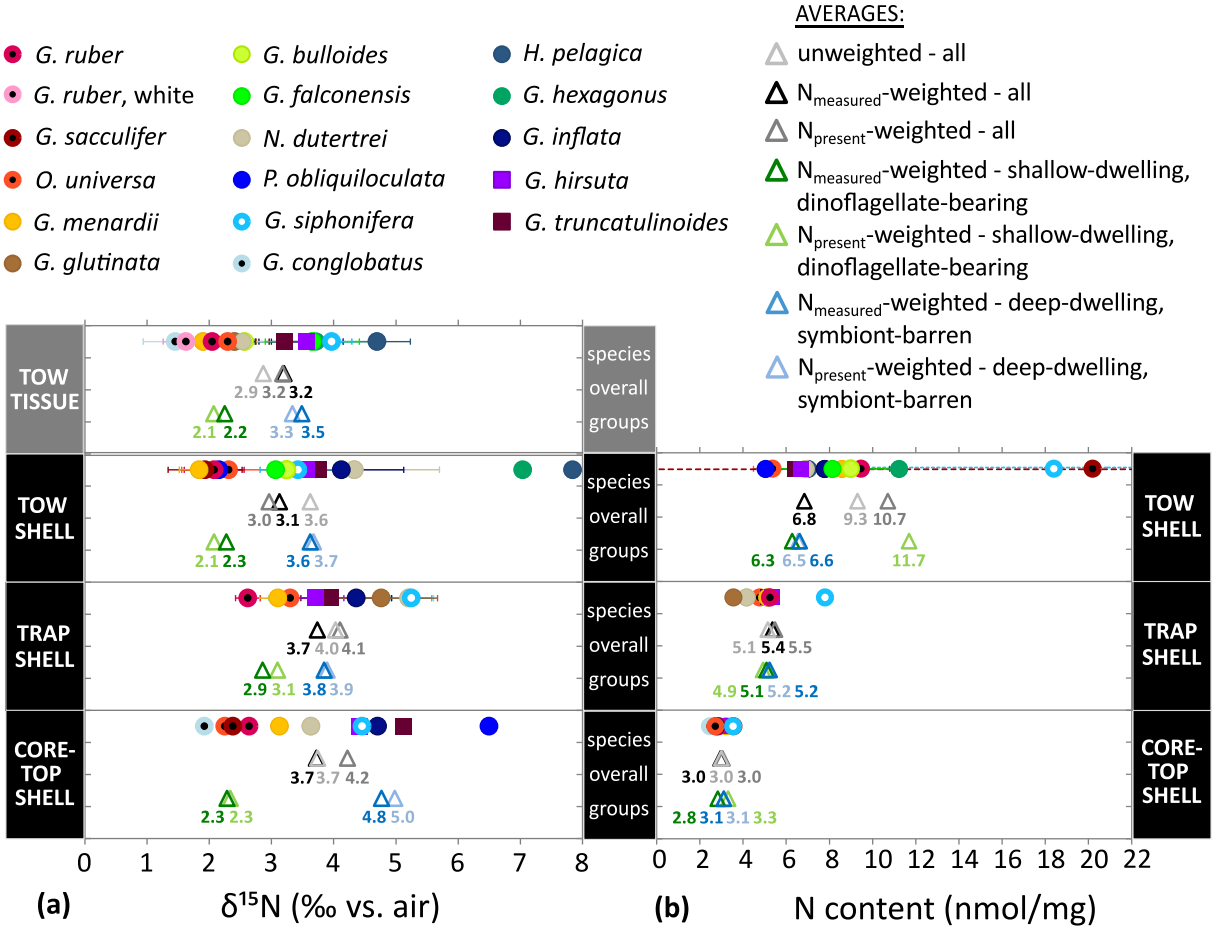

Fig. 2. Summary of the (a) $\delta^{15}N$ (in ‰ *vs.* N_2 in air) and (b) N content (in nmol/mg) of foraminifera collected from upper-ocean net tows (surface to 200 m), moored sediment traps (500 m, 1500 m and 3200 m) and core-top sediments (4570 m water depth) at the Bermuda Time-series Site. For each collection type, colored circles (shallow-to-intermediate dwellers) and squares (deep dwellers) show the average for each foraminifer species, with the fill color indicating the type of symbiont hosted (black fill for dinoflagellates, white fill for chrysophytes), if any symbiosis has been confirmed. Error bars show standard error (the standard deviation divided by the square root of the number of samples), and are dashed when overlap would otherwise obscure them. Black and grey triangles average over all species for each type of collection (light grey for unweighted averages; black where species are weighted by contribution to the total amount of N measured ($N_{measured}$-weighted); dark grey where species are weighted by contribution to the estimated amount of foraminiferal N (>100 μm) present in the environment ($N_{present}$-weighted); see section 2.3 for details). Green and blue triangles show group averages for dinoflagellate-bearing, shallow-dwellers and symbiont-barren, deep-dwelling species, respectively; bright green/blue for $N_{measured}$-weighted and pastel green/blue for $N_{present}$-weighted averages. For an expanded view of sinking shell-bound $\delta^{15}N$ (for the cases where we have measurements from multiple sediment trap depths), refer to Fig. A4. (For interpretation of the references to color in this figure legend, the reader is referred to the web version of this article.)

averages of 3.7‰ and 4.1‰ for $N_{measured}$ and $N_{present}$, respectively. Core-top shells (n = 11) range from 1.9‰ to 6.5‰ with an unweighted average $\delta^{15}N$ of 3.7‰, and weighted averages of 3.7‰ and 4.2‰ for $N_{measured}$ and $N_{present}$, respectively (Fig. 2a).

The N content of tow-collected shells (n = 72) generally ranges from 5.0 to 11.2 nmol/mg (except for *G. siphonifera* and *G. sacculifer*, which exceed 18 nmol/mg) with an unweighted average of 9.3 nmol/mg (Fig. 2b). Weighting species by contribution to $N_{measured}$ and $N_{present}$ yields averages of 6.8 nmol/mg and 10.7 nmol/mg, respectively. Sinking shells (n = 86) have a lower N content than tow-caught shells and a smaller range of 3.5 to 5.4 nmol/mg (with a higher value of 7.8 nmol/mg for *G. siphonifera*). On average, the N content of sinking shells is 5.1 nmol/mg (unweighted), 5.4 nmol/mg ($N_{measured}$-weighted) and 5.5 nmol/mg ($N_{present}$-weighted). Core-top shell N content (n = 11) has a still narrower range (2.5 to 3.5 nmol/mg) and lower average value (3.0 nmol/mg, both weighted and unweighted).

We begin by comparing the $\delta^{15}N$ of foraminiferal tissue with shell-bound $\delta^{15}N$ in the upper ocean and then present a time-series view of foraminifer-bound $\delta^{15}N$ to address whether this proxy captures the seasonal cycle and/or other temporal signals. Finally, we trace the journey of foraminifer shells as they sink through the water column, highlighting any changes in shell-bound $\delta^{15}N$ along the way.

3.2. Foraminifer tissue *vs.* shell-bound $\delta^{15}N$ from net tows

For most species, tissue $\delta^{15}N$ is similar between the two years of sampling, albeit with a tendency for lower average $\delta^{15}N$ in the first year (Fig. 3). This comparison suggests that, despite the potential for interannual variability and for biases associated with unavoidable irregularities in sampling schedule, our sampling and analyses have captured the characteristic $\delta^{15}N$ of the different species. A species-level comparison of all available data pairs (from a range of individual tows or cruises; n = 33) shows a pervasive positive correlation between tissue and shell-bound $\delta^{15}N$ (Fig. 4a). All species except *G. falconensis* exhibit positive regression slopes (Table 1), indicating that a large portion of shell-bound $\delta^{15}N$ variation is associated with variation in the $\delta^{15}N$ of foraminiferal tissue. Of the nine species with positive slopes, seven (or six when outliers are excluded)

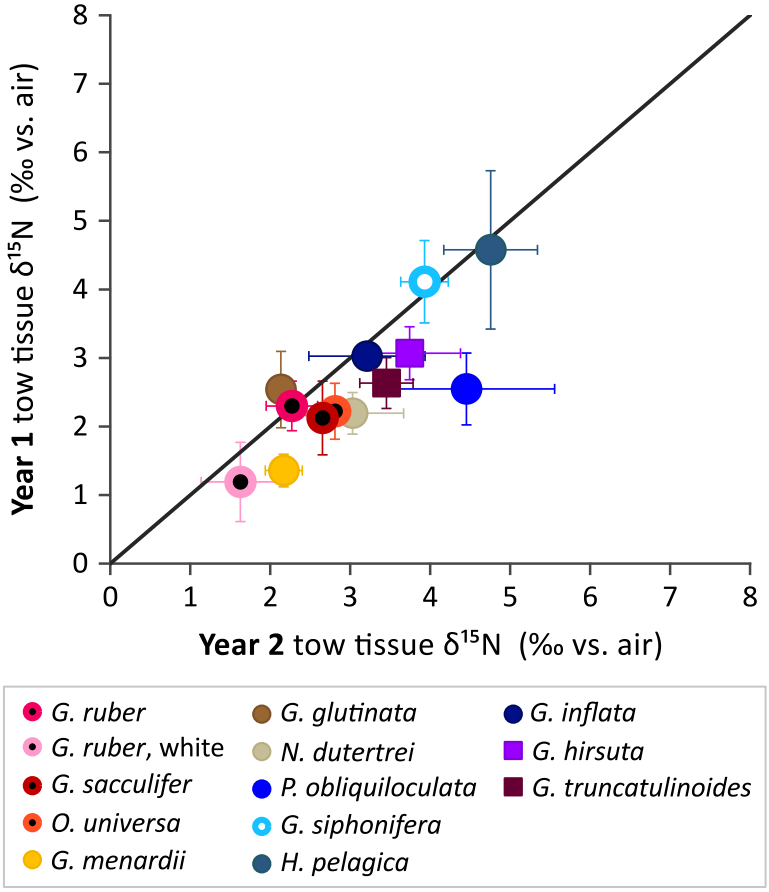

Fig. 3. Comparison of foraminifer tissue $\delta^{15}N$ for each species (colored circles and squares) between the two years of net tow sampling. Year 1 includes July 2011, October 2011, April 2012 and July 2012 (i.e., excludes February 2012), and Year 2 includes August 2012, November 2012, April 2013 and July 2013 (i.e., excludes November 2013) to ensure even seasonal coverage of both years. Error bars show standard error. (For interpretation of the references to colour in this figure legend, the reader is referred to the web version of this article.)

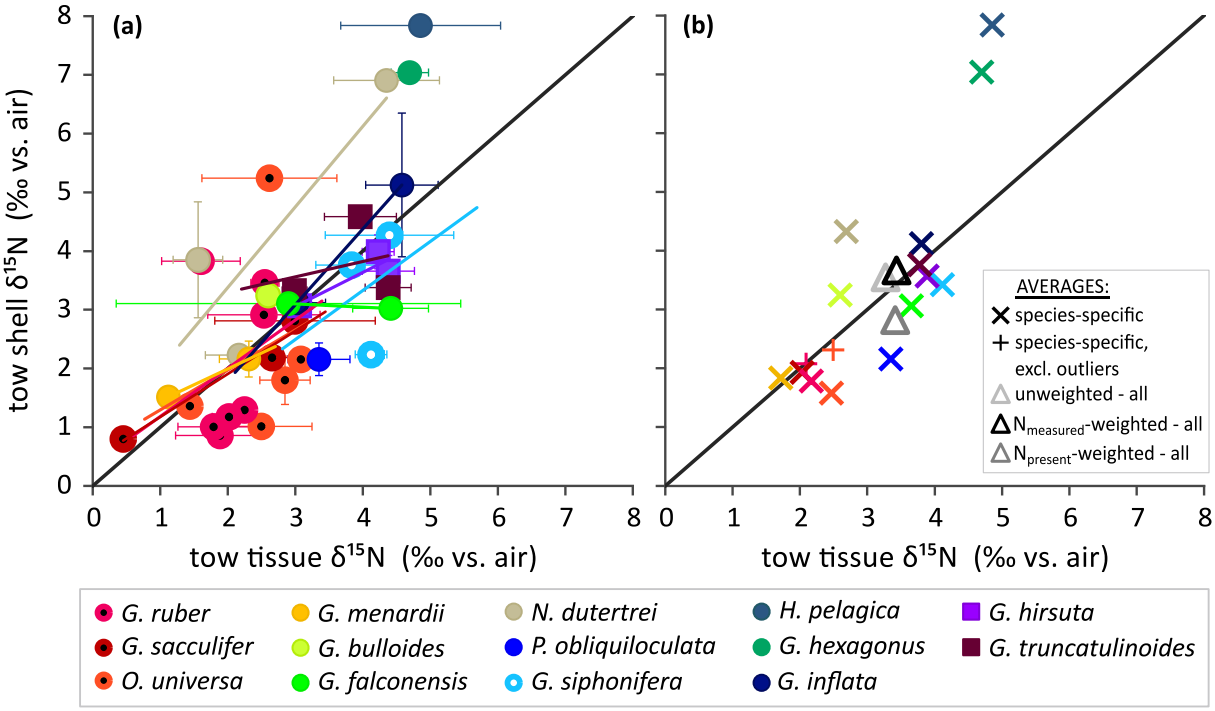

Fig. 4. Species-level comparison between foraminifer tissue $\delta^{15}N$ and corresponding shell-bound $\delta^{15}N$ from tow collections in the upper ocean (0–200 m), with 1:1 lines (black diagonals) for reference. (a) Simple regression lines (based on the monthly averages, i.e., the average of all measurements from all tows on a single cruise; colored circles and squares) are plotted for each species. Regression slopes and correlation coefficients, including and excluding outliers (one *O. universa* (orange) and one *G. ruber* (dark pink) measurement), are given in Table 1. Error bars in panel (a) show standard deviation. (b) Average tissue $\delta^{15}N$ *vs.* shell-bound $\delta^{15}N$ for each species, incorporating only the paired data shown in panel (a), including ('x' symbols) and excluding ('+' symbols) outliers. Triangles indicate overall averages; unweighted (light grey), $N_{measured}$-weighted (black) and $N_{present}$-weighted (dark grey). The large standard error (shown by the error bars in panel (a)) for some species derives mainly from $\delta^{15}N$ variability between cruises (rather than variability between measurements or variability between different tows from the same cruise). (For interpretation of the references to color in this figure legend, the reader is referred to the web version of this article.)

Table 1
Regression lines resulting from plotting tissue $\delta^{15}N$ (x-axis) *vs.* shell-bound $\delta^{15}N$ (y-axis) for each foraminifer species with $n \geq 2$ (see Fig. 3a).

	Regression line		
Species	slope	R^2	n
O. universa	0.68	0.06	5
– excluding outlier	0.41	0.35	4
G. ruber	0.82	0.06	7
– excluding outlier	3.10	0.84	6
G. sacculifer	0.73	0.97	3
G. siphonifera	0.83	0.05	3
N. dutertrei	1.37	0.72	3
G. hirsuta	0.58	0.80	3
G. inflata	1.29	(1.00)	2
G. menardii	0.54	(1.00)	2
G. truncatulinoides	0.26	0.07	3
G. falconensis	−0.06	(1.00)	2

have slopes less than 1, indicating greater $\delta^{15}N$ variability in tissue than in shell-bound N. Most species averages fall within 0.5‰ (*G. ruber*, *G. sacculifer*, *G. hirsuta*, *G. inflata*, *G. menardii*, *G. truncatulinoides*) or 1‰ (*O. universa*, *G. siphonifera*, *G. bulloides*, *G. falconensis*) of a 1:1 line in a plot of tissue *vs.* shell-bound $\delta^{15}N$, while others exhibit a 1-2‰ deviation above (*N. dutertrei*) or below (*P. obliquiloculata*) the 1:1 line (Fig. 4b). The most extreme deviations from 1:1 are observed for *H. pelagica* and *G. hexagonus*, with shell-bound $\delta^{15}N$ values 2-3‰ higher than their tissue. Nevertheless, both weighted (black and dark grey triangles) and unweighted averages of all species (light grey triangle) fall close to (i.e., within 0.6‰ of) the 1:1 line. On the whole, while there is a fair amount of scatter around a 1:1 relationship, there is no consistent offset between foraminifer tissue and shell-bound $\delta^{15}N$.

In histograms of the compiled $\delta^{15}N$ measurements (Fig. 5), a pattern common to both tissue and shell measurements is a clustering of *O. universa* (orange), *G. ruber* (dark pink) and *G. sacculifer* (dark red) at the lower end of the $\delta^{15}N$ distribution (typically < 3.5‰), and a clustering of *G. hirsuta* (purple), *G. truncatulinoides* (plum) and *G. inflata* (navy blue) at the higher end (typically > 3‰) (Fig. 5a and b). The $\delta^{15}N$ difference between these two groups is significant in both tissue and shell-bound N ($p \ll 0.05$ based on a two-sample, unequal variances *t*-test (Welch, 1947); see Table A3 for details). For other species (particularly *G. siphonifera* (sky blue) and *N. dutertrei* (tan)), measurements are more evenly distributed across a wide range of $\delta^{15}N$ values. Looking across seasons

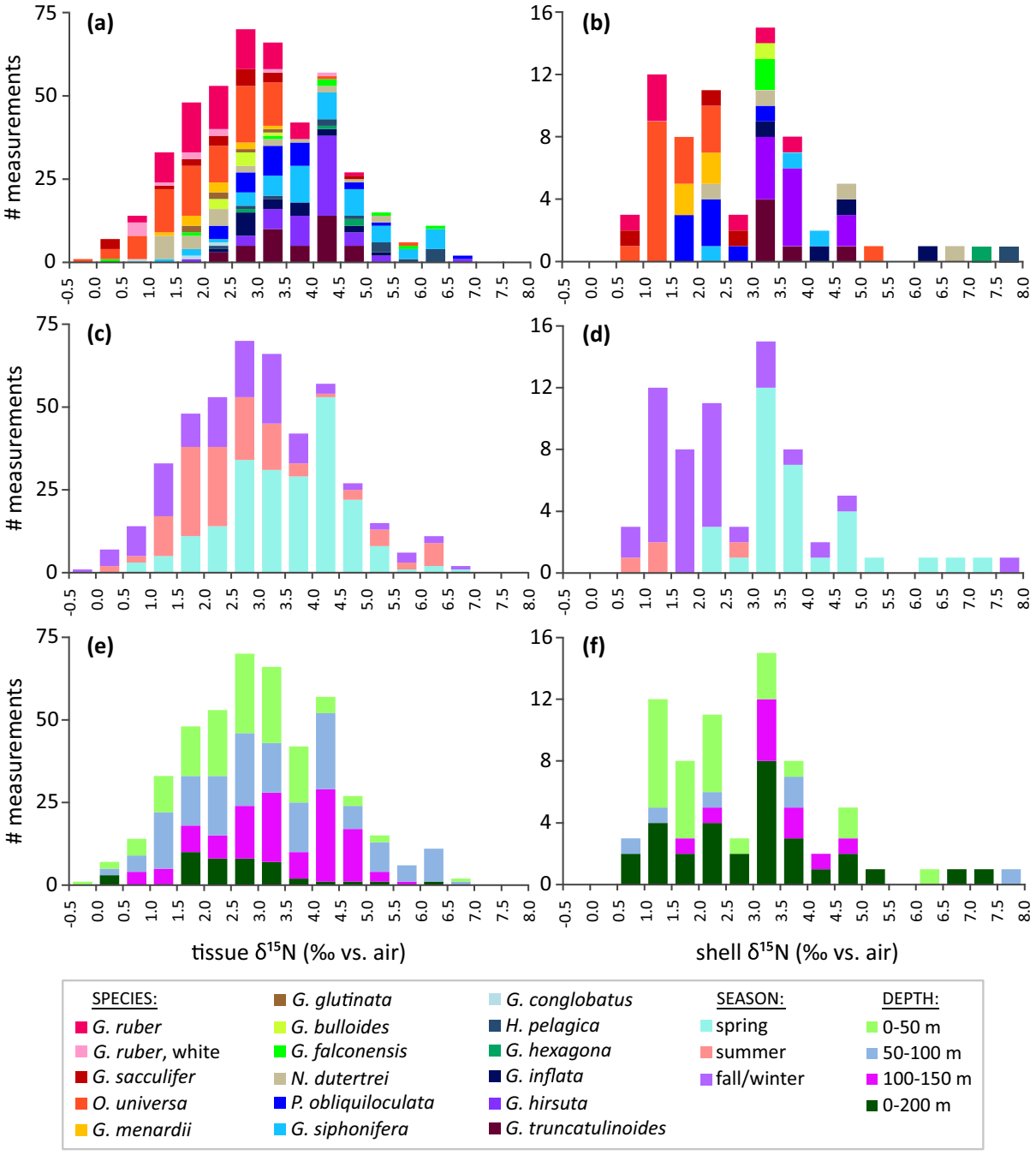

Fig. 5. Histograms showing the distribution of $\delta^{15}N$ measurements obtained from the tissue (a, c, e) and shells (b, d, f) of tow-collected foraminifera, colored by species (a, b), season (c, d) and collection depth (e, f). (For interpretation of the references to colour in this figure legend, the reader is referred to the web version of this article.)

(Fig. 5c and d), summer and fall $\delta^{15}N$ values are both significantly lower than springtime $\delta^{15}N$ and not statistically different from each other (Table A3). This pattern exists in both tissue $\delta^{15}N$ (averaging 2.7‰ and 2.6‰ *vs.* 3.5‰, respectively) and shell-bound $\delta^{15}N$ (averaging 1.5‰ and 2.1‰ *vs.* 3.9‰, respectively). The tissue $\delta^{15}N$ data also reveal significant increases with tow depth (Table A3), from an average of 2.7‰ at 0–50 m to 3.3‰ at 50–100 m and 3.4‰ at 100–150 m (Fig. 5e). While the pattern is less clear in the shell-bound measurements (for which different tow depths often had to be combined; 0–200 m category (dark green bars)), there is a significant increase between the 0–50 m and 100–150 m intervals (Table A3), averaging 2.4‰ and 3.4‰, respectively (Fig. 5f). Similarly, the $\delta^{15}N$ of size-fractionated (200–5000 μm) PON from these tows increases with depth, from an average of 3.2‰ at 0–50 m to 3.8‰ at 50–100 m to 4.2‰ at 100–150 m (where n = 31, 26, and 17, respectively; Fig. A1). In addition, the larger

PON size fractions are generally higher in $\delta^{15}N$ than the smaller size fractions (e.g., 2.7‰ (n = 16) for 200–500 μm and 4.4‰ (n = 21) for 2000–5000 μm PON, on average).

3.3. Time-series of $\delta^{15}N$ in foraminifera from sediment traps and net tows

In the foraminifer-bound $\delta^{15}N$ of sinking shells measured from fall 2009 to fall 2010, the dominant pattern that emerges for most species (*G. siphonifera*, *G. hirsuta*, *G. truncatulinoides*, *G. inflata*) is a $\delta^{15}N$ minimum in late winter/early spring (after the period of deepest mixing) followed by a $\delta^{15}N$ maximum in late spring (coinciding with the rapid shoaling of the mixed layer) (Fig. 6). Thereafter, the species for which we have data show a gradual decline in $\delta^{15}N$ over the course of the summer (as surface waters become increasingly thermally stratified), with a clear $\delta^{15}N$ offset between species (i.e., *O. universa* and *G. ruber* remaining ~2‰ lower than *G. siphonifera*). The $\delta^{15}N$ of bulk sinking PON collected in the sediment trap at 500 m shows a similar progression (with a minimum in early spring, a maximum in early summer and a gradual decline through the summer). While the $\delta^{15}N$ of bulk PON in the 500 m, 1500 m and 3200 m traps (ranging from −0.6‰ to 5.1‰) is generally lower than that of the foraminifer-bound fraction (0.8‰ to 6.6‰), the amplitude of the seasonal $\delta^{15}N$ change is very similar (5.7‰ *vs.* 5.8‰). The presence/absence of foraminifer species through the trap time-series is consistent with previous observations of seasonal changes in species composition in the Sargasso Sea (e.g., Bé, 1960; Deuser et al., 1981; Deuser, 1987; Salmon et al., 2015). While *G. ruber* and *G. siphonifera* occur throughout the year, *O. universa* shows a marked decrease in abundance during winter. *G. truncatulinoides*, *G. inflata* and *G. hirsuta* peak in winter and spring, while *N. dutertrei* is confined to a brief period in winter or spring (the latter in our case). The scarcity of *H. pelagica* in sinking and seafloor material (despite being one of the most abundant species in surface waters year-round) is likely due to extensive structural weakening of their monolamellar and thin-walled tests during gametogenesis, which reduces their preservation (Deuser et al., 1981).

The time-series of upper-ocean net tow samples (tissue and shell-bound $\delta^{15}N$) from summer 2011 to fall 2013 (Fig. A2) shows a similar range of $\delta^{15}N$ variability to the sinking shells (varying by ~5–6‰ overall) and exhibits similar relationships between species (e.g., *O. universa* and *G. ruber* at the lower end and *G. siphonifera* at the upper end of the foraminifer $\delta^{15}N$ spectrum). Roughly in parallel with the sediment trap observations, the $\delta^{15}N$ of tow-collected PON (>200 μm) also peaks in late spring and declines in late summer, illustrated here by the 200–1000 μm fraction from the upper 0–100 m (thick, mauve line in Fig. A2) (mostly copepods in the Bermuda region; Deevey and Brooks, 1971). While the timing of response across different foraminifer species in the net tows is not as consistent as for sinking shells, the $\delta^{15}N$ of most net tow foraminifer species varies in concert with the $\delta^{15}N$ of tow-collected PON.

Fig. A3 shows the $\delta^{15}N$ of nitrate (and nitrate + nitrite) at 200 m and 250 m water depth (near the base of the thermocline), spanning both tow and trap sampling periods (Fawcett et al., 2011, 2014, 2015). These data indicate no significant nitrate (or nitrate + nitrite) $\delta^{15}N$ difference between the two periods ($p > 0.05$ based on a two-sample, unequal variances *t*-test; Welch, 1947) with a $\delta^{15}N$ of 2.6 ± 0.2‰ (2.5 ± 0.2‰) during the trap period (n = 6) and a $\delta^{15}N$ of 2.6 ± 0.1‰ (2.5 ± 0.2‰) during the tow period (n = 20).

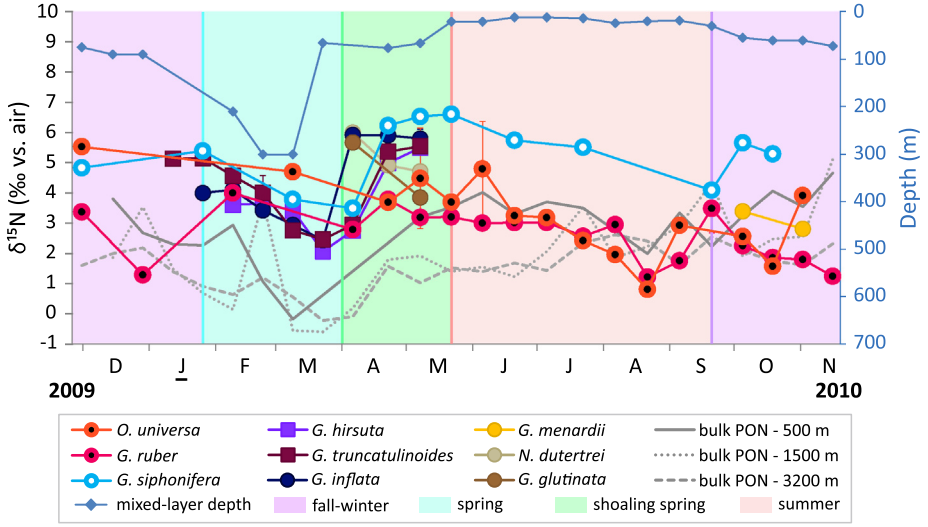

Fig. 6. Time-series of foraminifer-bound $\delta^{15}N$ (colored circles and squares) collected in sediment traps (moored at 500 m, 1500 m and 3200 m) between November 2009 and November 2010. Where more than one measurement was possible, error bars show standard deviation. The $\delta^{15}N$ of bulk PON collected in each trap over the same period is also shown (dashed and dotted lines). Mixed layer depth (blue diamonds) is plotted on the secondary y-axis, and background colors denote seasons (blue for spring, green for shoaling spring, pink for summer, purple for fall/winter). (For interpretation of the references to color in this figure legend, the reader is referred to the web version of this article.)

3.4. Shell-bound $\delta^{15}N$ from net tows to sediment traps and the seafloor

Comparison between foraminifer-bound $\delta^{15}N$ of shells from upper ocean net tows (collected between July 2011 and November 2013) and those collected in sediment traps (between November 2009 and November 2010) shows sinking shells to be elevated in $\delta^{15}N$ by 0.1‰ to 1.8‰ (Fig. 7a). This elevation appears to be species-dependent. While some species (*G. hirsuta*, *G. truncatulinoides*, *G. inflata*) show almost no offset (falling within 0.2‰ of the 1:1 line), on average, trap-caught shells are between 0.6‰ (using $N_{measured}$) and 1.3‰ (using $N_{present}$) higher in $\delta^{15}N$ than tow-caught shells (as indicated by the deviations of the triangle symbols from the 1:1 line). The $\delta^{15}N$ difference between tow- and trap-collected shells is strongly significant ($p \ll 0.05$; based on a two-sample, unequal variances *t*-test; Welch, 1947), regardless of whether (or with which method) measurements are weighted by N contribution ($n = 61–94$ for tow shells and $n = 77–92$ for trap shells). Between 500 m and 3200 m (the depth interval spanned by the three OFP traps), there is no change evident in the $\delta^{15}N$ of sinking shells, except for *O. universa*, which increases by ~2‰ (Fig. A4). Comparison of foraminifer-bound $\delta^{15}N$ of sinking shells with that of shells from core-top sediments shows no consistent offset from the 1:1 line (Fig. 7b). The $\delta^{15}N$ offset ranges from −1.6‰ to 1.2‰, with an unweighted average of 0.1‰ (light grey triangle) and weighted averages of −0.1‰ (black triangle) and −0.3‰ (dark grey triangle), for $N_{measured}$ and $N_{present}$, respectively. We note that the average offsets reported here differ slightly from the offsets implied by the triangles in summary Fig. 2a. This is because the triangles in Fig. 2 average over all available data, not only those species for which we have paired (x, y) measurements (as in Fig. 7a and b).

4. DISCUSSION

4.1. Relationship between foraminifer tissue and shell-bound $\delta^{15}N$ in the upper subtropical ocean

On the whole, there is no systematic offset in $\delta^{15}N$ between tissue and shell-bound N in living foraminifera at the Bermuda Time-series Site (Fig. 4). This implies that the compounds used by foraminifera for shell building are not isotopically distinct from their bulk tissue. A similarity in $\delta^{15}N$ has been observed between the coral-bound N and tissue of symbiotic corals (Muscatine et al., 2005), but not in diatoms, where frustule-bound $\delta^{15}N$ differs substantially from diatom tissue $\delta^{15}N$ (Sigman et al., 1999b; Horn et al., 2011; Morales et al., 2013; Morales et al., 2014). This difference may be due to the fact that the N bound within foraminifer tests and coral skeletons is mainly comprised of amino acids (King and Hare, 1972; Drake et al., 2017), a significant constituent of the tissue, whereas the organic N in diatom frustules is largely composed of long-chain

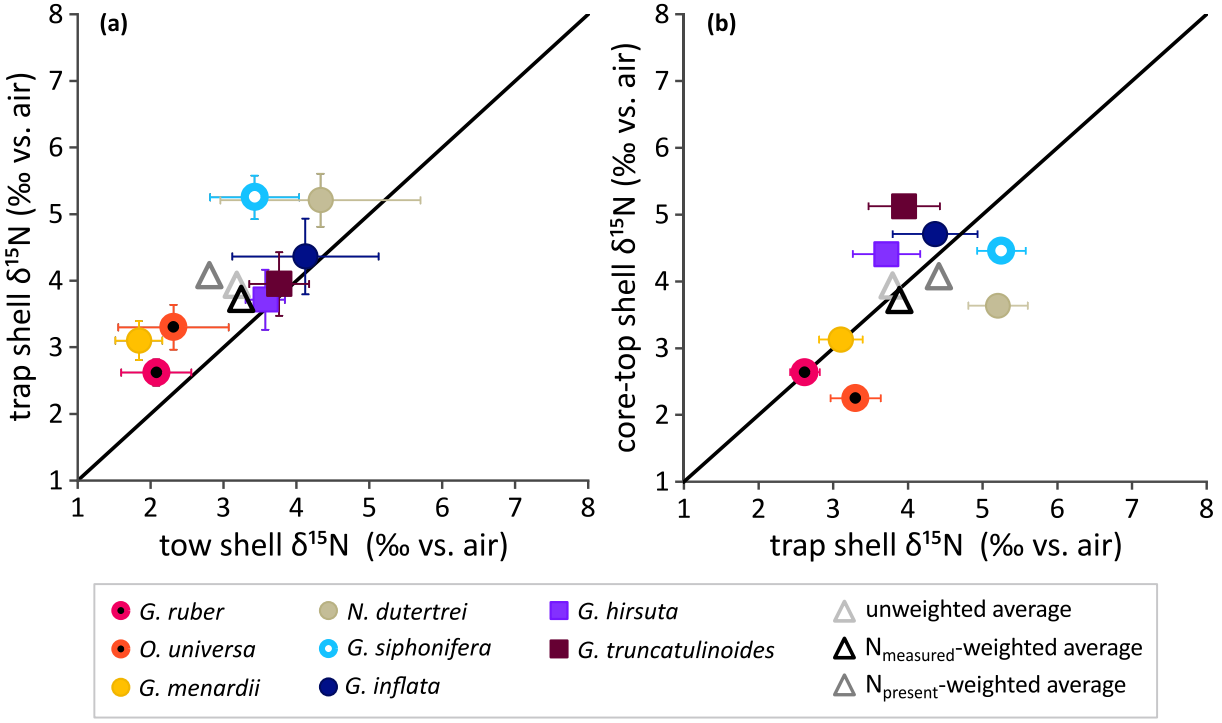

Fig. 7. Changes in foraminifer-bound $\delta^{15}N$ through the water column as revealed through a comparison of the $\delta^{15}N$ of (a) tow-caught *vs.* sinking shells and (b) sinking *vs.* core-top shells. Colored circles and squares represent species averages, and triangles mark the weighted (black and dark grey) and unweighted (light grey) averages over all species shown in a panel. Standard error is shown by error bars, except for core-top shell $\delta^{15}N$ (the y-axis in panel (b)), for which measurements derive from a single collection (i.e., the seasonal $\delta^{15}N$ range is unknown). (For interpretation of the references to colour in this figure legend, the reader is referred to the web version of this article.)

polyamines (Kröger et al., 2000; Sumper et al., 2005), specialized compounds for building opal frustules that are not widely used in the bulk tissue. Thus, differences in the $\delta^{15}N$ of biosynthetic compounds might produce an offset in $\delta^{15}N$ between diatom frustule-bound N and diatom tissue, whereas this is not expected for foraminifera and other calcifiers. A significant offset would increase the range of mechanisms by which the tissue/fossil $\delta^{15}N$ relationship might vary through time, and variation in this relationship would greatly complicate interpretation of paleo-proxy records. Thus, it is both practically convenient and fundamentally beneficial that foraminiferal tissue and shell-bound $\delta^{15}N$ are not distinctly different. At the same time, given the variability that we observe in this study, more work on this question is called for.

While the $\delta^{15}N$ relationship between foraminifer shell and tissue N appears to be characterized by a relatively high degree of variability, inter-season variation in foraminiferal tissue $\delta^{15}N$ is positively correlated with variation in shell $\delta^{15}N$ for all species for which we have adequate data to undertake the comparison (Fig. 4a). From this we conclude that most of the variation in shell-bound $\delta^{15}N$ has the same cause as tissue $\delta^{15}N$ variation (discussed below). For most species, we observe slopes that are less than 1, implying a greater $\delta^{15}N$ range in tissue than in shells. This observation is consistent with shell-bound N integrating over the lifetime of the organism (i.e., weeks to months), while tissues like cytoplasm (including food-containing vacuoles) record recent activity, allowing for greater variation between individuals of the same species living in the same environment. Details aside, the positive correlation and lack of a pervasive $\delta^{15}N$ offset between shell-bound and tissue N are auspicious for the foraminifer paleo-proxy, as they suggest that the $\delta^{15}N$ of organic matter trapped within fossil shells (as long as it is preserved) largely reflects the $\delta^{15}N$ of the organism over the course of its life.

4.2. Factors affecting foraminifer tissue and shell-bound $\delta^{15}N$

From the distributions of net tow $\delta^{15}N$ measurements (Fig. 5), it emerges that species, season, and depth play a role in determining foraminifera tissue and shell-bound $\delta^{15}N$. The dominant $\delta^{15}N$ distinction is between the spinose, dinoflagellate-bearing shallow dwellers, which dominate the lower end of the $\delta^{15}N$ range (*O. universa* (orange), *G. ruber* (dark pink) and *G. sacculifer* (dark red); Fig. 5a and b), and the non-spinose, non-dinoflagellate-bearing deeper dwellers, which tend to be higher in $\delta^{15}N$ (*G. hirsuta* (purple) and *G. truncatulinoides* (plum)). A similar $\delta^{15}N$ offset (of 0.5–2.0‰) between these two groups of species has previously been observed in sinking and core-top shells (Ren et al., 2012). Our data confirm an upper ocean origin for this signal. Two potential mechanisms were put forward by Ren et al. (2012) to explain the group-specific $\delta^{15}N$ difference. First, the lower $\delta^{15}N$ of spinose, euphotic zone-dwelling foraminifera (despite their dietary preference for high-$\delta^{15}N$ zooplankton) may result from their dinoflagellate symbionts consuming (and therefore reducing the excretion of) low-$\delta^{15}N$, metabolically produced ammonium. Second, the higher $\delta^{15}N$ of non-spinose, deeper-dwelling foraminifera (despite being predominantly herbivorous) may reflect their partial dependence on subeuphotic-zone PON, the $\delta^{15}N$ of which increases with depth (Fig. A1) (Altabet, 1988). Intermediate-dwelling species (including the spinose, chrysophyte-hosting *G. siphonifera* (sky blue) and the non-spinose (possibly chrysophyte-bearing) *N. dutertrei* (tan), *P. obliquiloculata* (blue) and *G. inflata* (navy)), exhibit a range of $\delta^{15}N$ values intermediate between the low-$\delta^{15}N$ dinoflagellate-bearing and high-$\delta^{15}N$ symbiont-barren groups, but most occupy a higher $\delta^{15}N$ range, more similar to the symbiont-barren species.

The $\delta^{15}N$ in foraminiferal tissue and shells in summer/fall tends to be lower than in spring (Fig. 5c and d). This may reflect the advantage that some symbiont-bearing foraminifera have under the oligotrophic conditions of seasonal (e.g., summertime in the mid-latitudes) or near-permanent (as in the tropics and subtropical gyres) stratification. Photosynthesising endosymbiotic algae use metabolized N forms (mostly ammonium) respired by their host and fix them into amino acids that are then available to foraminifera for biosynthesis. Consistent with this explanation, previous work indicates that dinoflagellate symbionts are primarily sustained by ammonium from the host foraminifer (Uhle et al., 1999). A similar observation has been made for symbiotic corals, which also appear to be low-productivity specialists (Muscatine et al., 2005). Thus, the shallow, well-lit mixed layers and low euphotic-zone nutrient concentrations at the Bermuda Time-series Site in late summer provide favourable growth conditions for dinoflagellate-bearing, surface-dwelling species (Tolderlund and Bé, 1971). This seasonality in on-site production (although modulated by current-transported tests) is reflected in the seasonality of shell fluxes in the OFP sediment traps. For example, the dinoflagellate-bearing *G. ruber* and *G. sacculifer* peak between July and October (Salmon et al., 2015), whereas fluxes of the symbiont-barren deep-dwellers (*G. truncatulinoides* and *G. hirsuta*) and (possibly chrysophyte-bearing) intermediate-dwellers (*G. inflata* and *N. dutertrei*) peak in late winter and spring, respectively, when phytoplankton production and export (and thus food availability) are at a maximum (Lomas et al., 2013; Salmon et al., 2015). In addition to the seasonal shift in the dominant foraminifer group (i.e., from symbiont-barren to dinoflagellate-bearing), enhanced symbiotic activity of (and thus reduced efflux of low-$\delta^{15}N$ ammonium from) dinoflagellate-bearing species may contribute to the spring-to-summer decline in foraminifer $\delta^{15}N$ for a given species. However, at least part of this summertime species-specific $\delta^{15}N$ decline must be due to the observed decrease in the baseline $\delta^{15}N$ of available food sources (Fig. A2). Seasonality is examined further in Section 4.3.

The data indicate an increase in the $\delta^{15}N$ of foraminiferal tissue (and to a lesser extent, shells) with depth within the upper 150 m (Fig. 5e and f). Depth stratification has been observed previously in foraminifer species distributions and in their shell carbon and oxygen isotopic compositions (Fairbanks et al., 1980; Fairbanks et al., 1982; Ravelo and Fairbanks, 1992; Mulitza et al., 1997; Mulitza et al., 2004). Thus, one might suspect that the observed

$\delta^{15}N$ increase derives from partitioned depth habitats, with lower-$\delta^{15}N$ dinoflagellate-bearing species dominating the euphotic zone and higher-$\delta^{15}N$ symbiont-barren/chryso phyte-bearing species dwelling deeper in the water column. However, the common occurrence of "deep-typical" *G. truncatulinoides* and *G. hirsuta* in shallow tow collections and "shallow-typical" *G. ruber* and *O. universa* in deeper tow collections argues against strong partitioning of species over this depth interval, particularly when averaged over the year. Indeed, many of the species analyzed here have overlapping depth habitats within the upper 150 m (e.g., *O. universa* and *G. bulloides*), and others undergo large depth changes during ontogeny (e.g., *G. truncatulinoides*). Therefore, collection depth should not be expected to represent the primary depth habitat. Rather, the depth gradient in the $\delta^{15}N$ of bulk suspended (>0.7 μm) PON below ~100 m in the Sargasso Sea (Saino and Hattori, 1980; Altabet, 1988), as well as in the larger (>200 μm) PON size fractions measured here (increasing by ~1.0‰ between the surface and 150 m; Fig. A1) suggest that the ~0.9‰ increase in foraminifer tissue over the same interval may reflect an increase in the $\delta^{15}N$ of their diet.

An alternative (but not necessarily contradictory) hypothesis for the observed group-specific $\delta^{15}N$ differences is that different species have distinct compositions of amino acids (King and Hare, 1972; Stathoplos and Hare, 1989; Robbins and Brew, 1990), which undergo varying degrees of isotopic fractionation during synthesis and/or translocation (Uhle et al., 1997; McClelland and Montoya, 2002). For instance, the apparently greater trophic enrichment of symbiont-barren foraminifera compared to dinoflagellate-bearers might be explained as deriving from a greater proportion of "trophic" (e.g., glutamic acid) *vs.* "source" (e.g., phenylanaline) amino acids (Popp et al., 2007; McCarthy et al., 2007) in the symbiont-barren group. While the existing amino acid content data from core-top planktic foraminifera do not support this interpretation (King and Hare, 1972; Robbins and Brew, 1990), amino-acid-specific $\delta^{15}N$ measurements would help to robustly test this.

As implied by the histograms (Fig. 5), averaging across euphotic zone-dwelling, dinoflagellate-bearing species (green triangles in Fig. 2a) yields a lower $\delta^{15}N$ than averaging across deeper-dwelling, symbiont-barren species (blue triangles in Fig. 2a). The resulting group averages reveal similar shell *vs.* tissue $\delta^{15}N$ relationships: the shells of both euphotic zone, dinoflagellate-bearing species and deep-dwelling, symbiont-barren species are only 0.1‰ elevated relative to their respective tissues. From this observation, we infer that the organic components employed by both symbiont-bearing and symbiont-barren foraminifera in biomineralization resemble their respective bulk tissues in amino acid composition. In this way, foraminifera may differ from corals: Muscatine et al. (2005) found that symbiont-barren corals exhibit a significantly higher $\delta^{15}N$ for skeletal N than for tissue N while symbiont-bearing corals do not.

4.3. Seasonal signals in foraminifer-bound $\delta^{15}N$

Here, we consolidate and extend our discussion of the seasonality of foraminifer-bound $\delta^{15}N$ and its underlying drivers. While our tow collections exhibit modest seasonal variation in $\delta^{15}N$ (with foraminifer tissue, shell-bound, and bulk PON $\delta^{15}N$ generally being lowest in late summer/fall and highest in spring), the trend in sinking shells is more apparent (compare Fig. 6 with Fig. A2). This is not surprising, as sediment traps remain in place year-round, sampling at regular intervals and integrating over longer timescales (~14 days) than net tows. By contrast, 120–190 min net tows only provide a snapshot of foraminifer $\delta^{15}N$, and thus capture shorter term variations and small-scale features (e.g., storms, short-lived eddies or filaments) that may blur or overwhelm the seasonal signal (Schiebel et al., 1995; Beckmann et al., 1987; Schmuker and Schiebel, 2002).

The $\delta^{15}N$ of sinking shells shows a distinctive minimum in late winter/early spring (Fig. 6). This follows closely after the period of deepest mixing (down to ~300 m in late February 2010), when deep nitrate is supplied to surface waters and the $\delta^{15}N$ of nitrate is 'reset' to the thermocline value (~2.6‰; Fig. A3) (Knapp et al., 2005; Fawcett et al., 2015). The late-spring maximum in foraminifer-bound $\delta^{15}N$ follows the rapid shoaling of the mixed layer (to ~ 20 m in May 2010) and the peak of the spring phytoplankton bloom (Lomas et al., 2013). During this time, nitrate in surface waters is drawn down rapidly, driving an increase in the $\delta^{15}N$ of the nitrate pool being consumed (due to isotopic fractionation during nitrate assimilation) (Knapp et al., 2005; Fawcett et al., 2015) and thus also the $\delta^{15}N$ of any PON subsequently produced from it (Altabet et al., 1991; Sigman et al., 1999a). Given that all foraminifera consume a component of the PON pool, it seems reasonable that shell-bound $\delta^{15}N$ in sinking shells also records this $\delta^{15}N$ increase (depicted by panels 1–2 in Fig. 8). In short, even though it was not our intention to focus on seasonal nitrate drawdown at this study of a subtropical gyre site, this signal was recovered.

The decrease in $\delta^{15}N$ observed in sinking shells through the summer and fall coincides with the period of intense stratification when the nitrate supply from below is severely impeded (Steinberg et al., 2001; Lomas et al., 2013). Previous studies have found this to be a period of enhanced recycling of N within the shallow mixed layer (Menzel and Ryther, 1960; Lipschultz, 2001). Because recycled ammonium is lower in $\delta^{15}N$ than nitrate (Checkley and Miller, 1989; Lehmann et al., 2002), as the phytoplankton community becomes more dependent on ammonium, the $\delta^{15}N$ of PON suspended in the euphotic zone (including eukaryotic phytoplankton (Fawcett et al., 2014) and thus also the zooplankton that prey upon them) decreases (Fig. A2). Foraminifera, representing a subset of the zooplankton in the system, would also be expected to record this signal, explaining the decrease in shell-bound $\delta^{15}N$ during the summer and fall (as illustrated in panels 2–3 of Fig. 8). Thus, the data argue that the shells of individual foraminifer species capture seasonal changes in the $\delta^{15}N$ of phytoplankton and zooplankton biomass. At the same time, there is evidence for enhanced internal N cycling within the foraminifer-dinoflagellate system during late spring and summer from the changing $\delta^{15}N$ offset between dinoflagellate-bearing *vs.* symbiont-barren species, as well as between dinoflagellate-bearing species and their food

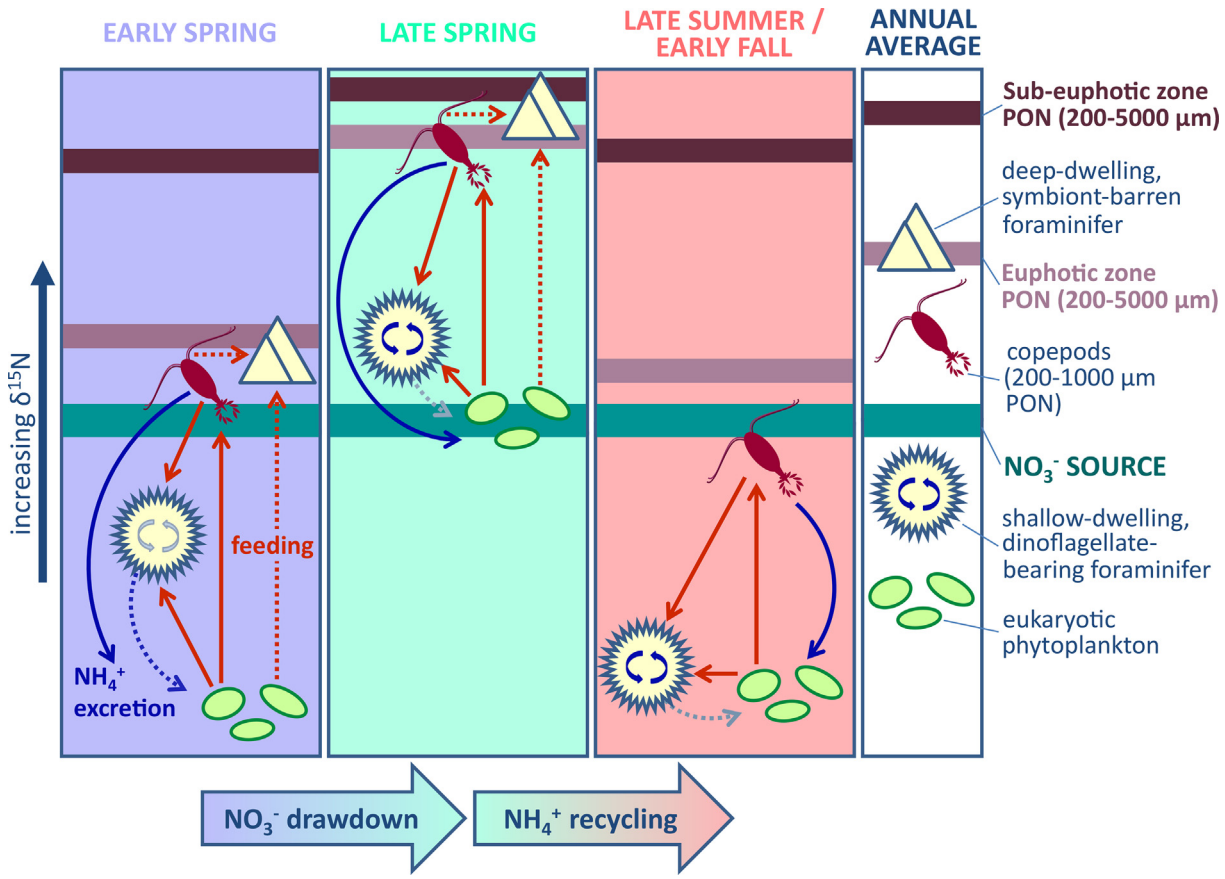

Fig. 8. Cartoon depicting the seasonal progression in $\delta^{15}N$ (panels 1–3) and the annual average state (panel 4) of dinoflagellate-bearing/shallow-typical and symbiont-barren/deep-typical foraminifera in relation to copepods, eukaryotic phytoplankton (both primary components of the sinking flux) and the mean annual nitrate supply to the euphotic zone at the Bermuda Time-series Site. Red arrows indicate feeding (solid arrows indicating preference for fresh prey, dashed arrows indicating consumption of detrital particles and/or the organisms that feed upon them), which raises the $\delta^{15}N$ of the heterotroph relative to their diet. Blue arrows indicate ammonium excretion, which lowers the $\delta^{15}N$ of the phytoplankton that assimilate this ammonium. Circular arrows inside the shallow-typical foraminifer represents internal ammonium recycling between the host and photosymbionts, which lowers the $\delta^{15}N$ (and trophic level) of the host when active (with the activity indicated by the darkness of the cyclic arrows). (For interpretation of the references to color in this figure legend, the reader is referred to the web version of this article.)

sources (Fig. 8). In February/March, the sinking shells of dinoflagellate-bearing *G. ruber* and *O. universa* are similar in $\delta^{15}N$ to those of symbiont-barren species (e.g., *G. truncatulinoides*) (Fig. 6). By the end of April, *O. universa* and *G. ruber* shell-bound $\delta^{15}N$ have decreased slightly, despite sharp $\delta^{15}N$ increases in their primary food sources: copepods (200–1000 µm PON in Fig. 8 and Fig. A2) and eukaryotic phytoplankton (Fawcett et al., 2014). The resulting divergence of *O. universa* and *G. ruber* $\delta^{15}N$ below that of symbiont-barren foraminifera (by 1–3‰ in late spring; Fig. 6) may thus reflect more active or efficient retention of low-$\delta^{15}N$ ammonium within the host-symbiont system under improving light conditions of a shallower mixed layer (Fig. 8). Evaluating this possibility further might be pursued by measuring the $\delta^{15}N$ relationship between the symbionts and foraminifer host tissue on a seasonal basis.

Curiously, we also observe a significant $\delta^{15}N$ offset (2–3‰) between sinking shells of *G. ruber* / *O. universa* and *G. siphonifera* in early spring and summer, despite all three species being symbiont-bearing and largely carnivorous (Fig. 6). However, by late fall through early spring, this $\delta^{15}N$ difference is no longer apparent. This may represent additional evidence that the chrysophyte symbiosis of *G. siphonifera* is not as active in N cycling as the dinoflagellate symbioses of *G. ruber* and *O. universa* (Hemleben et al., 1989; Spero, 1998; Bijma et al., 1998), such that *G. siphonifera* is more similar in its N isotope characteristics to symbiont-barren foraminifera. If this is the case, the convergence of $\delta^{15}N$ in *G. ruber*/*O. universa* and *G. siphonifera* in late fall to early spring could result from a decrease in activity of host-dinoflagellate recycling, effectively raising the trophic levels (and thus shell-bound $\delta^{15}N$) of *G. ruber* and *O. universa* during this period. However, an additional consideration is that *G. siphonifera* has two genotypes, each with a different type of chrysophyte symbiosis: type I (facultative) and type II (obligatory) (Faber et al., 1988; Faber et al., 1989; Bijma et al., 1998). The two are morphologically similar (and thus were not separated here), but exhibit distinct growth, feeding and reproductive behavior

(Faber et al., 1988; Faber et al., 1989). In the future, types I and II should be measured separately (at least from net tow collections) to evaluate their contributions (if different) to the observed seasonal signal in *G. siphonifera* $\delta^{15}N$.

4.4. Changes in shell-bound $\delta^{15}N$ with depth

An important consideration for the application of the foraminifer $\delta^{15}N$ paleo-proxy is whether the $\delta^{15}N$ of foraminifer-bound N changes as a test sinks through the water column and is ultimately incorporated into the seafloor sediments. Between the net tows in the upper 200 m of the water column and the sediment traps at mid-depths, the $\delta^{15}N$ of shells increases by 0.6‰, while the N content decreases by 1.4 nmol/mg ($N_{measured}$-weighted averages; black triangles in Fig. 7a and b). Between the sediment traps and the seafloor, shell N content continues to decrease by an average of 2.4 nmol/mg, while average $\delta^{15}N$ remains unchanged. Below, we consider potential reasons for these observations.

4.4.1. Alteration in the upper water column

There are several possible explanations for the $\delta^{15}N$ rise from the tows to the traps: environmental differences between the two sampling periods, addition to or alteration of the test structure or composition during gametogenesis, and alteration of shell-bound N during early diagenesis (with or without shell dissolution and the associated exposure of previously protected organic N). In the available nitrate + nitrite data (Fig. A3) (Fawcett et al., 2011, 2014, 2015), we observe no significant $\delta^{15}N$ difference ($p > 0.05$) between the two sampling periods (July 2011–November 2013 for the tows and November 2009–November 2010 for the traps), nor from the $\delta^{15}N$ of nitrate + nitrite (2.65 ± 0.32‰) at 250 m between June 2000 and May 2001 (Knapp et al., 2005). These data argue that a difference in the $\delta^{15}N$ of the N supply to the euphotic zone is not responsible for the observed difference in foraminifer-bound $\delta^{15}N$ between net tow- and sediment trap-collected shells.

The remaining possible explanations for the tow-to-trap $\delta^{15}N$ difference would have implications for fossil foraminifer $\delta^{15}N$ as a paleo-proxy. First, the tow-to-trap $\delta^{15}N$ increase might result from alteration during gametogenesis, the final stage of a foraminifer's life cycle. During this stage, some species migrate to a different depth in the water column and may form gametogenic calcite (and/or additional chambers) before releasing their gametes into the surrounding water (Deuser et al., 1981; Deuser, 1987; Schiebel et al., 1997a; Schiebel et al., 2002). Even within the same species, the degree of gametogenic calcification may vary substantially between specimens (Hemleben et al., 1989; Schiebel and Hemleben, 2017). Shallow-dwelling species like *O. universa* typically descend to the deep chlorophyll maximum (near the base of the euphotic zone at the Bermuda Time-series Site) for reproduction, while deep-dwellers like *G. truncatulinoides* and *G. hirsuta* ascend and proliferate in near-surface waters in early spring (Schiebel et al., 2002; Schiebel and Hemleben, 2005). If the gametogenic calcite encapsulates organic N with a $\delta^{15}N$ that is different from that of the shell-bound N laid down during the foraminifer's juvenile and adult life, this might explain at least part of the difference in foraminifer-bound $\delta^{15}N$ between net tow and sediment trap collections. Because gametogenic calcification (unlike chamber building) does not require a new structural template, the added calcite lacks the N-rich primary organic sheet of ontogenic calcite. While very little is known about the distribution of non-laminar organics in gametogenic calcite (Branson et al., 2016), we generally expect this calcite to be organic-poor and thus to contribute to the decline in shell N content from tows to traps.

However, our N content data combined with previously published data on the mass and/or thickness of gametogenic calcite do not make a compelling case for gametogenesis as the main explanation for the tow-to-trap differences in shell-bound N content or $\delta^{15}N$. Given that gametogenic calcite typically contributes 4–20% of the mass in post-gametogenic *O. universa* shells (Hamilton et al., 2008), the observed decrease in N content from tows to traps (from 5.4 nmol/mg to 4.8 nmol/mg, respectively) would require gametogenic calcite to have an N content of −9.9 to +1.8 nmol/mg. The negative concentrations are physically impossible and thus indicate that the mass of added calcite is generally too low for it to explain the N content decrease. Similarly, *N. dutertrei* (with an average gametogenic layer that is 46% of the total shell-wall thickness (Steinhardt et al., 2015), and assuming a range of ±10%) would require the added calcite to have an N content of −3.5 to −0.7 nmol/mg to reproduce the observed N content decline (from 6.9 to 4.2 nmol/mg). For the remaining four species with sufficient data to undertake the calculation (all *Globoratalids*), we assume the thickness of gametogenic calcite in *Globorotalia scitula* shells (47% (Steinhardt et al., 2015), ±10%) to be a reasonable approximation. Of these four, only *G. truncatulinoides* and *G. hirsuta* yield non-negative N contents (between 1.7 and 3.0 nmol/mg). From the calculated N contents, the $\delta^{15}N$ of gametogenic calcite in these two species is inferred to be between 5.2 and 7.9‰. It is unclear why gametogenic calcite would have a $\delta^{15}N$ so different from the rest of the shell and tissue. As with the N content calculations, this argues against the gametogenic calcite N as the driver of the changes from net tows to sediment traps. These apparent failings of an explanation focused on gametogenesis compel us to consider N loss from shells (or the shell assemblage) during early diagenesis.

If a low-$\delta^{15}N$ N pool were preferentially lost from sinking shells post-mortem, it would leave the remaining shell-bound N elevated in $\delta^{15}N$. As foraminifer tests sink, any external (i.e., non-calcified) N is accessible (to bacteria, predators, etc.) and the $\delta^{15}N$ of the remaining tissue is vulnerable to alteration. Indeed, the preferential removal of ^{14}N during decomposition is thought to drive the observed increase in the $\delta^{15}N$ of bulk suspended PON with depth in the Sargasso Sea (Saino and Hattori, 1980; Altabet and McCarthy, 1986; Altabet, 1988). However, before foraminifer-bound $\delta^{15}N$ measurements are made, the tests undergo harsh chemical cleaning (see Section 2.2) to ensure that any accessible and potentially compromised organic matter is removed (Ren et al., 2009). Thus, the tow-to-trap increase in foraminifer-bound $\delta^{15}N$ is not easily

explained by bacterially-mediated diagenesis of the foraminifer-native N. It is possible that shell-bound organic matter degrades chemically, without being exposed to environmental fluids and bacterial processes. Indeed, such degradation very likely occurs. As a well-documented example, biomineral matrix-bound amino acids racemize over time, with impacts on the proteins in which they occur (Bada, 1982; Collins et al., 1998). However, it seems unlikely that such degradation would provide a mechanism by which the associated N would be released from the mineral matrix, absent changes in the mineral matrix itself. Thus, especially with regard to the changes in shell-bound N from net tow- to sediment trap-collected foraminifera, we focus our attention on diagenesis of the mineral matrix that protects the shell-bound N.

Partial dissolution of settling foraminifer shells may be an important process. It is evident from the size distribution of sinking and sedimentary tests (compared with living fauna) that larger, faster-sinking tests are preferentially preserved over smaller, slower-sinking tests (Peeters et al., 1999). The shells of juveniles are thinly calcified (Fehrenbacher et al., 2017) and have not yet undergone ontogenetic and/or gametogenic thickening, such that the larger shells of foraminifera that have completed their life cycle are preferentially preserved through the water column and into the sediments (Schiebel and Hemleben, 2017; and references therein). Moreover, substantial (19%) weight loss in shells of the same size has been observed between 100 m and 1000 m depth in the North Atlantic, despite the supersaturated state of calcite in ambient seawater and the addition of gametogenic calcite (Schiebel et al., 2007). One explanation is that, as exposed organic tissues (including cytoplasm and any organic coatings, e.g., pore linings) are decomposed by bacteria post mortem, weak organic acids are released, creating a micro-environment within and/or surrounding the test that is conducive to dissolution (i.e., under-saturated with respect to calcite) (Schiebel et al., 1997b; Milliman et al., 1999; Schiebel, 2002; Schiebel et al., 2007; Schiebel and Hemleben, 2017). Alternatively, this shallow dissolution might entail the loss of vaterite, the unstable (and more soluble) polymorph of calcium carbonate, as its protective organic membrane decays post mortem (Jacob et al., 2017).

For any of these scenarios to explain our observations, the dissolution would need to expose N-bearing organic matter with a low $\delta^{15}N$ to diagenetic loss, causing shell-bound N to rise in $\delta^{15}N$ as its N content declines. If dissolution alone were responsible for the tow-to-trap differences in $\delta^{15}N$ and N content of shell-bound N, the $\delta^{15}N$ of the lost organic matter would need to be approximately 2.2‰ lower than that of tow-collected shells. If the smaller, thinly calcified (thus, high N content) shells of all species are the main casualties of upper water column dissolution, the low $\delta^{15}N$ implied for smaller shells might reflect the lower trophic level of juveniles (feeding more on small phytoplankton and less on copepod zooplankton) relative to adults. At the same time, weight loss in shells of the same size class (observed by Schiebel et al., 2007) indicates partial dissolution of the shells that do survive sinking through the upper water column. Indeed, shells collected below this zone often show signs of dissolution within chambers of the final whorl (e.g., peeling of the chamber wall and corroded pores; Constandanche et al., 2013). The outermost (and normally the largest) chambers are generally more vulnerable to dissolution and breakage, as they are not as sheltered as the innermost chambers. Thus, if the largest (most recently formed) chambers and/or their inner walls are the primary sites of dissolution in the upper 500 m, we might infer that the low $\delta^{15}N$ of constituent organic matter reflects an increasing reliance on symbiont photosynthesis toward the end of the foraminiferal life span (i.e., enhanced cyclic N flow). This is consistent with the observed strong correlation between test size and symbiont density (Spero and Parker, 1985), in that it may require greater retention of low-$\delta^{15}N$ ammonium within the host-symbiont system to support the increasing photosynthetic rates of dinoflagellates as the foraminifer grows. Repeating the above calculation, but separating species by symbiotic state, reveals that the $\delta^{15}N$ of calcite lost from the dinoflagellate-bearing group is notably lower than their tow shell average (−0.2‰ and 2.3‰, respectively), while the $\delta^{15}N$ of calcite lost from the symbiont-barren group is only slightly lower than their average (2.8‰ and 3.6‰). This distinction is also evident from paired measurements (where only species appearing in both tows and traps are compared; Fig. 7a): while symbiont-bearing species are offset by 0.5–1.8‰ above the 1:1 line, symbiont-barren species (*G. hirsuta* (purple), *G. truncatulinoides* (plum)) fall only slightly (by 0.1–0.2‰) above the 1:1 line. These observations may indicate the preferential dissolution of the most recently formed chambers from dinoflagellate-hosting foraminifera, bearing the strongest low-$\delta^{15}N$ imprint of symbiont N cycling, as the main driver of the tow-to-trap $\delta^{15}N$ increase.

4.4.2. Preservation in the sediments

The average foraminifer-bound $\delta^{15}N$ of core-top sediments is nearly identical to sinking shells (Fig. 2a), despite a further 2.4 nmol/mg decrease in N content (Fig. 2b) from sinking to burial, with this transition representing a much longer period of time than from living to sinking. During this phase, there is no net effect on shell-bound $\delta^{15}N$. Passive encrustation of shells is unlikely to incorporate much organic matter and thus represents a possible mechanism for lowering N content. However, substantial shell weight gain by encrustation is unlikely (Lohmann, 1995). For such overgrowth alone to explain the 45% decrease in average N content from traps to core-tops, an increase in shell weight of at least an 80% would be required. Yet shell-weight data show neither a consistent increase nor decrease (Takahashi and Bé, 1984). Thus, the best explanations for the N content decrease are (1) the dissolution of N-rich shells or N-rich portions of shells, or (2) chemical degradation of the shell-bound organic matter that then somehow ends its protection by the mineral matrix.

Close inspection of the trap-to-seafloor change in shell-bound $\delta^{15}N$ suggests a distinction between the $\delta^{15}N$ of calcite lost from symbiont-bearing and symbiont-barren species, with the dinoflagellate-bearing group losing N with a higher $\delta^{15}N$ than their sinking shell average (3.6‰ and

2.9‰, respectively), while the $\delta^{15}N$ of calcite lost from the symbiont-barren group appears to be lower than their average (2.5‰ and 3.8‰, respectively). This weak distinction, if real, may reflect the interaction between changes in the $\delta^{15}N$ of calcite-bound N added during growth with the differential vulnerability of different parts of the shell (or shells of different size and/or maturity) to dissolution on the seafloor. In general, though, our essential finding is that seafloor alteration appears to have only very minor effects on shell-bound $\delta^{15}N$.

4.4.3. Overview of depth changes

In summary, the observations discussed above suggest a role for dissolution-driven N loss as shells sink through the water column and are incorporated into the sediments. In the early phase, as shells sink through the upper 500 m, low-$\delta^{15}N$ calcite is lost, perhaps because this calcite derives from the lowest-$\delta^{15}N$ chambers of dinoflagellate-bearing foraminifera. Gametogenic thickening (which is expected to add low-N calcite) might contribute to the decrease in the average N content of shells from net tows to sediment traps, but cannot explain the entire change. In the deeper water column and sediments, a second phase of dissolution appears to remove calcite that is less isotopically distinct from shell-bound N as a whole. Most likely, the two phases of dissolution-driven N loss are continuous, with the loss of the most dissolution-prone calcite/vaterite (e.g., small, slowly-sinking, perhaps cytoplasm-containing tests, as well as the outermost chambers of individual tests) transitioning gradually to dissolution of calcite that is less distinct from that of the total shell assemblage. Future measurements of the organic N in separate size fractions and specific shell components (e.g., ontogenic *vs.* gametogenic calcite) would help to test the explanations proposed here.

5. IMPLICATIONS FOR THE FORAMINIFER-BOUND $\delta^{15}N$ PALEO-PROXY

Given the near-complete consumption of nitrate in Sargasso Sea surface waters, the mean annual $\delta^{15}N$ of living foraminifera in this environment should converge on the $\delta^{15}N$ of the nitrate supply. Indeed, we find the annually-averaged $\delta^{15}N$ (weighted by $N_{measured}$) of the bulk tissue (3.2‰) and shell-bound N (3.1‰) from tow-caught foraminifera to be within 0.6‰ of shallow thermocline (~200 m) nitrate (2.6‰). The individual species reveal two distinct groupings. Dinoflagellate-bearing, euphotic zone-dwelling foraminifera have tissue $\delta^{15}N$ (2.2‰) and shell-bound $\delta^{15}N$ (2.3‰) that are similar to the $\delta^{15}N$ of the annual nitrate supply from the thermocline. In contrast, symbiont-barren, deep-dwelling foraminifera record a higher $\delta^{15}N$ than thermocline nitrate for both tissue and shell-bound N (3.5‰ and 3.6‰, respectively). A potential concern is the subsequent rise in shell-bound $\delta^{15}N$ by 0.6‰ on average (weighted by $N_{measured}$) as foraminifera sink through the upper water column. Further work is called for to address whether this $\delta^{15}N$ increase is robust and widespread or variable. Despite the changes that occur as foraminifer shells sink and settle on the seafloor, the distinction between low-$\delta^{15}N$ euphotic zone-dwelling, dinoflagellate-bearing and high-$\delta^{15}N$ deeper-dwelling, symbiont-barren species holds throughout the water column and into the sediments (compare green *vs.* blue triangles from surface tows with deeper sinking and core-top values; Fig. 2a). Thus, knowledge of the basic ecology of the chosen foraminifer species is important for accurately inferring past nitrate $\delta^{15}N$ from downcore fossil shells.

Time-series of foraminifer $\delta^{15}N$ appear to follow the seasonal variation in $\delta^{15}N$ of autotrophic biomass and PON in general. This is consistent with the expectation that foraminifera acquire most, if not all, of their N from feeding and not directly from the nitrate supply. On a seasonal basis, PON $\delta^{15}N$ varies for reasons other than the $\delta^{15}N$ of the nitrate supply, including the isotopically fractionating drawdown of nitrate in the spring and the onset of intense N cycling in the late summer and early fall, and foraminifer $\delta^{15}N$ appears to track these seasonal PON $\delta^{15}N$ changes. This raises the concern that, at times in the past, foraminifer $\delta^{15}N$ might stray from the current relationship with subsurface nitrate $\delta^{15}N$ if, for example, N recycling in surface waters was more or less important (relative to nitrate-based production). This basic concern is inherent in any proxy that tracks a component of the PON in the upper ocean or in the sinking flux, as opposed to the integrated sinking flux itself. Only the integrated N export is ensured by mass balance to record the $\delta^{15}N$ of the nitrate consumed in the euphotic zone.

We have shown here that, despite an imprint of N recycling on the seasonality of foraminifera, the shell-bound $\delta^{15}N$ of the euphotic zone-dwelling, dinoflagellate-bearing foraminifera approximates the $\delta^{15}N$ of the mean annual nitrate supply, as has been found at other sites based mostly on foraminifer shells from surface sediments (Ren et al., 2009; Ren et al., 2012). This supports the expectation that, at least for the subtropical ocean, the $\delta^{15}N$ of the nitrate consumed in the euphotic zone (equivalent to the annual nitrate supply) is the underlying control on foraminifer-bound $\delta^{15}N$. The isotopic similarity between foraminifera (especially the dinoflagellate-bearing, shallow-dwellers) and the annual mean nitrate supply is consistent with their typical reliance on zooplankton and eukaryotic phytoplankton as their prey (Fig. 8). Eukaryotic phytoplankton and small zooplankton together appear to account for most of the sinking flux at the Bermuda Time-series Site (Fawcett et al., 2011), so that their consumption by foraminifera should tie the annually-integrated foraminifer $\delta^{15}N$ to the $\delta^{15}N$ of export production. The linkage exists despite the isotopic fractionation during N metabolism that causes heterotrophs to be higher in $\delta^{15}N$ than their prey. This isotopic fractionation also returns low-$\delta^{15}N$ ammonium to surface waters, which drives a compensatory decline in phytoplankton $\delta^{15}N$, eventually lowering the $\delta^{15}N$ of zooplankton as well (Fig. 8). Over the annual cycle, the net effect is for the $\delta^{15}N$ of grazing zooplankton to approximate that of the sinking flux, as long as heterotrophs are responsible for most of the N export; our data and previous measurements are consistent with this view of the system. In the case of dinoflagellate-bearing foraminifera, their consumption of both eukaryotic phytoplankton and heterotrophs weakens the significance of any isotopic distinctions between the two, potentially making

these species a particularly reliable measure of the $\delta^{15}N$ of the N export in the subtropical ocean.

On the whole, our findings also bode well for the implementation of the foraminifer-bound $\delta^{15}N$ paleo-proxy at high latitudes. We argue above that foraminifera in most environments should record variations in the $\delta^{15}N$ of upper-ocean PON and of the sinking flux. In polar regions, these isotopic properties will respond to changes in both the $\delta^{15}N$ of the subsurface nitrate supply and the degree of nitrate consumption by phytoplankton. At the same time, the evidence for a role of upper ocean N recycling in the seasonality of foraminifer $\delta^{15}N$ raises the possibility that the effect of recycling on foraminifera $\delta^{15}N$ may be important in paleoceanographic studies of polar ocean regions, which appear to have undergone large changes in nitrate supply and export production over time. Changes in the $\delta^{15}N$ offset between different foraminifer species have been observed (Ren et al., 2015), and the seasonally varying processes of nitrate drawdown and N recycling may be responsible. Ground-truthing of the foraminifer-bound $\delta^{15}N$ proxy in the modern polar ocean will be critical for identifying and testing such possibilities.

ACKNOWLEDGEMENTS

The data presented in this study can be found at http://www.bco-dmo.org.

This work was supported by NSF grants OCE-1060947, 0960802, and 1136345 (D.M.S.); Taiwan MOST grant 105-2628-M-002-007-MY3 (H.R.); the South African National Antarctic Programme (grant 93069, A. Roychoudhury; grant 105539, S.E.F.); the South African NRF CSUR fund (grant 105895, S.E.F); the Max Planck Institute for Chemistry, Germany, and the South African NRF (grant 111090, S.M.S.). We thank the US NSF Chemical Oceanography Program for their continued support of the BATS and OFP time-series, most recently by grants OCE-0752366 (BATS) and OCE-1536644 (OFP). We are grateful to the staff of the Bermuda Institute of Ocean Sciences, the captain and crew of the R/V *Atlantic Explorer*, as well as fellow scientists for assistance in sampling and auxiliary data collection. We thank A. Plattner for assistance with creating Fig. 1 (in GMT; Wessel et al., 2013); as well as H. Spero for the helpful discussions. S.M.S. thanks the Department of Earth and Environmental Sciences at Fresno State as host, for providing a welcoming and productive academic environment, and A. Roychoudhury for his continued guidance and support.

APPENDIX A. SUPPLEMENTARY MATERIAL

Supplementary data associated with this article can be found, in the online version, at https://doi.org/10.1016/j.gca.2018.05.023.

REFERENCES

Altabet M. A. (1988) Variations in nitrogen isotopic composition between sinking and suspended particles: implications for nitrogen cycling and particle transformation in the open ocean. *Deep-Sea Res. Pt I* **35**, 535–554.

Altabet M. A. and Curry W. B. (1989) Testing models of past ocean chemistry using foraminifera $^{15}N/^{14}N$. *Global Biogeochem. Cycles* **3**(2), 107–119.

Altabet M. A. and François R. (1994) Sedimentary nitrogen isotopic ratio as a recorder for surface ocean nitrate utilization. *Global Biogeochem. Cycles* **8**(1), 103–116.

Altabet M. A. and McCarthy J. J. (1986) Vertical patterns in ^{15}N natural abundance in PON from the surface waters of warm-core rings. *J. Mar. Res.* **44**, 185–201.

Altabet M. A., Deuser W. G., Honjo S. and Stienen S. (1991) Seasonal and depth-related changes in the source of sinking particles in the N Atlantic. *Nature* **354**, 136–139.

Bada J. L. (1982) Racemization of amino acids in nature. *Interdiscipl Sci. Rev.* **7**(1), 30–46.

Bé A. W. H. (1960) Ecology of recent planktonic foraminifera: Part 2: bathymetric and seasonal distributions in the Sargasso Sea Off Bermuda. *Micropaleontology* **6**(4), 373–392.

Bé A. W. H., Hemleben C., Anderson O. R., Spindler M., Hacunda J. and Tuntivate-Choy S. (1977) Laboratory and field observations of living planktonic foraminifera. *Micropaleontology* **23** (2), 155–179.

Bé A. W. H., Hemleben C., Anderson O. R. and Spindler M. (). *Chamber formation in planktonic foraminifera* **25**(3), 294–307.

Beckmann W., Auras A. and Hemleben C. (1987) Cyclonic cold-core eddy in the eastern North Atlantic III. Zooplankton. *Mar. Ecol. Prog. Ser.* **39**, 165–173.

Bijma J., Hemleben C., Huber B. T., Erlenkeuser H. and Kroon D. (1998) Experimental determination of the ontogenetic stable isotope variability in two morphotypes of Globigerinella siphonifera (d'Orbigny). *Mar. Micropaleontol.* **35**, 141–160.

Braman R. S. and Hendrix S. A. (1989) Nanogram nitrite and nitrate determination in environmental and biological materials by Vanadium(III) reduction with chemiluminescence detection. *Anal. Chem.* **61**, 2715–2718.

Branson O., Bonnin E. A., Perea D. E., Spero H. J., Zhu Z., Winters M., Hönisch B., Russell A. D., Fehrenbacher J. S. and Gagnon A. C. (2016) Nanometer-scale chemistry of a calcite biomineralization template: implications for skeletal composition and nucleation. *Proc. Natl. Acad. Sci.* **113**(46), 12934–12939.

Casciotti K. L., Sigman D. M., Galanter Hastings M., Böhlke J. K. and Hilkert A. (2002) Measurement of the oxygen isotopic composition of nitrate in seawater and freshwater using the denitrifier method. *Anal. Chem.* **74**, 4905–4912.

Checkley D. M. and Miller C. A. (1989) Nitrogen isotope fractionation by oceanic zooplankton. *Deep-Sea Res. Pt A* **36**, 1449–1456.

CLIMAP Project Members (1981). Seasonal reconstruction of the Earth's surface at the last glacial maximum. Geol. Soc. Am., Map and Chart Series, 1–18.

CLIMAP Project Members, 1994. CLIMAP 18K Database. IGBP PAGES/ World Data Center-A for Paleoclimatology Data Contribution Series # 94-001. Available online: <ftp://ftp.ncdc.noaa.gov/pub/data/paleo/paleocean/climap/climap18/>.

Collins M. J., Walton D. and King A. (1998). Nitrogen-containing macromolecules in the bio- and geosphere. ACS Symposium Series, vol. 707. American Chemical Society. Chap. The Geochemical Fate of Proteins, pages 74–87.

Constandanche M., Yerly F. and Spezzaferri S. (2013) Internal pore measurements on macroperforate planktonic foraminifera as an alternative morphometric approach. *Swiss J. Geosci.* **106**, 179–186.

Conte M. H. and Weber J. C. (2014) Particle flux in the deep Sargasso Sea: The 35-year Oceanic Flux Program time series. *Oceanography* **27**(1), 142–147.

Conte M. H., Ralph N. and E. Ross E. (2001) Seasonal and interannual variability in deep ocean particle fluxes at the Oceanic Flux Program/Bermuda Atlantic Time-series (BATS) site in the western Sargasso Sea near Bermuda. *Deep-Sea Res. Pt II* **48**, 1471–1505.

de Boyer Montégut C., Madec G., Fischer A. S., Lazar A. and Iudicone D. (2004) Mixed layer depth over the global ocean: An examination of profile data and a profile-based climatology. *J. Geophys. Res.* **109**(C12003).

Deevey G. B. and Brooks A. L. (1971) The annual cycle in quantity and composition of the zooplankton of the Sargasso Sea off Bermuda. 2. The surface to 2000 m. *Limnol. Oceanogr.* **16**(6), 927–943.

Deuser W. G. (1987) Seasonal variations in isotopic composition and deep-water fluxes of the test of perennially abundant planktonic foraminifera of the Sargasso Sea: results from sediment-trap collections and their paleoceanographic significance. *J. Foramin. Res.* **17**(1), 14–27.

Deuser W. G., Ross E. H., Hemleben C. and Spindler M. (1981) Seasonal changes in species composition, numbers, mass, size, and isotopic composition of planktonic foraminifera settling into the deep Sargasso Sea. *Palaeogeogr. Palaeoclimatol. Palaeoecol.* **33**, 103–127.

Drake J. L., Schaller M. F., Mass T., Godfrey L., Fu A., Sherrell R. M., Rosenthal Y. and Falkowski P. G. (2017) Molecular and geochemical perspectives on the influence of CO_2 on calcification in coral cell cultures. *Limnol. Oceanogr.*, 1–15.

Faber W. W., Anderson O. R., Lindsey J. L. and Caron D. A. (1988) Algal-foraminiferal symbiosis in the planktonic foraminifer Globigerinella aequilateralis: I. Occurrence and stability of two mutually exclusive chrysophyte endosymbionts and their ultrastructure. *J. Foramin. Res.* **18**, 334–343.

Faber W. W., Anderson O. R. and Caron D. A. (1989) Algal-foraminiferal symbiosis in the planktonic foraminifer Globigerinella aequilateralis: II. Effects of two symbiont species on foraminiferal growth and longevity. *J. Foramin. Res.* **19**(3), 185–193.

Fairbanks R. G., Wiere P. H. and Bé A. W. H. (1980) Vertical distribution and isotopic composition of living planktonic foraminifera in the Western North Atlantic. *Science* **207**(4426), 61–63.

Fairbanks R. G., Sverdlove M., Free R., Wiebe P. H. and Bé A. W. H. (1982) Vertical distribution and isotopic fractionation of living planktonic foraminifera from the Panama Basin. *Nature* **298**, 841–844.

Fawcett S. E., Lomas M. W., Casey J. R., Ward B. B. and Sigman D. M. (2011) Assimilation of upwelled nitrate by small eukaryotes in the Sargasso Sea. *Nat. Geosci.* **4**, 717–722.

Fawcett S. E., Lomas M. W., Ward B. B. and Sigman D. M. (2014) The counterintuitive effect of summer-to-fall mixed layer deepening on eukaryotic new production in the Sargasso Sea. *Global Biogeochem. Cycles* **28**, 86–102.

Fawcett S. E., Ward B. B., Lomas M. W. and Sigman D. M. (2015) Vertical decoupling of nitrate assimilation and nitrification in the Sargasso Sea. *Deep-Sea Res. Pt I* **103**, 64–72.

Fehrenbacher J. S., Russell A. D., Davis C. V., Gagnon A. C., Spero H. J., Cliff J. B., Zhu Z. and Martin P. (2017) Link between light-triggered Mg-banding and chamber formation in the planktic foraminifera Neogloboquadrina dutertrei. *Nat Commun*, 8.

François R., Altabet M. A. and Burckle L. H. (1992) Glacial to interglacial changes in surface nitrate utilization in the Indian sector of the Southern Ocean as recorded by sediment $\delta^{15}N$. *Paleoceanography* **7**(5), 589–606.

Gastrich M. D. (1987) Ultrastructure of a new intracellular symbiotic alga found within planktonic foraminifera. *J. Phycol.* **23**, 623–632.

Haidar A. T., Thierstein H. R. and Deuser W. G. (2000) Calcareous phytoplankton standing stocks, fluxes and accumulation in Holocene sediments off Bermuda (N. Atlantic). *Deep-Sea Res. Pt II* **47**, 1907–1938.

Hamilton C. P., Spero H. J., Bijma J. and Lea D. W. (2008) Geochemical investigation of gametogenic calcite addition in the planktonic foraminifera Orbulina universa. *Mar. Micropaleontol.* **68**, 256–267.

Hemleben C., Spindler M. and Anderson O.R. (1989). Modern Planktonic Foraminifera. Springer-Verlag.

Honjo S. and Erez J. (1978) Dissolution rates of calcium carbonate in the deep ocean; an in-situ experiment in the North Atlantic Ocean. *Earth Planet. Sci. Lett.* **40**(2), 287–300.

Horn M. G., Robinson R. S., Rynearson T. A. and Sigman D. M. (2011) Nitrogen isotopic relationship between diatom-bound and bulk organic matter of cultured polar diatoms. *Paleoceanography* **26**(PA3208).

Jacob D. E., Wirth R., Agbaje O. B. A., Branson O. and Eggins S. M. (2017) Planktic foraminifera form their shells via metastable carbonate phases. *Nat. Commun.*, 8.

King, Jr., K. and Hare P. E. (1972) Amino acid composition of the test as a taxonomic character for living and fossil planktonic foraminifera. *Micropaleontology* **18**(3), 285–293.

Knapp A. N., Sigman D. M. and Lipschultz F. (2005) N isotopic composition of dissolved organic nitrogen and nitrate at the Bermuda Atlantic Time-series Study site. *Global Biogeochem. Cycles* **19**, 1–15.

Kröger N., Deutzmann R., Bergsdorf C. and Sumper M. (2000) Species-specific polyamines from diatoms control silica morphology. *Proc. Natl. Acad. Sci. USA* **97**(26), 14133–14138.

Lehmann M. F., Bernasconi S. M., Barbieri A. and McKenzie J. A. (2002) Preservation of organic matter and alteration of its carbon and nitrogen isotope composition during simulated and in situ early sedimentary diagenesis. *Geochim. Cosmochim. Acta* **66**(20), 3573–3584.

Lipschultz F. (2001) A time-series assessment of the nitrogen cycle at BATS. *Deep-Sea Res. Pt II* **48**, 1897–1924.

Lohmann G. P. (1995) A model for variation in the chemistry of planktonic foraminifera due to secondary calcification and selective dissolution. *Paleoceanography* **10**(3), 445–457.

Lomas M. W., Bates N. R., Johnson R. J., Knap A. H., Steinberg D. K. and Carlson C. A. (2013). Two decades and counting: 24-years of sustained open ocean biogeochemical measurements in the Sargasso Sea. Deep-Sea Res. Pt II.

McCarthy M. D., Benner R., Lee C. and Fogel M. L. (2007) Amino acid nitrogen isotopic fractionation patterns as indicators of heterotrophy in plankton, particulate, and dissolved organic matter. *Geochimica et Cosmochimica Acta* **71**, 4727–4744.

McClelland J. W. and Montoya J. P. (2002) Trophic relationships and the nitrogen isotopic composition of amino acids in plankton. *Ecology* **83**(8), 2173–2180.

Meckler A. N., Ren H., Sigman D. M., Gruber N., Plessen B., Schubert C. J. and Haug G. H. (2011) Deglacial nitrogen isotope changes in the Gulf of Mexico: evidence from bulk sedimentary and foraminifera-bound nitrogen in Orca Basin sediments. *Paleoceanography* **26**(PA4216), 1–13.

Menzel D. W. and Ryther J. H. (1960) The annual cycle of primary production in the Sargasso Sea off Bermuda. *Deep Sea Res.* **6**, 351–367.

Milliman J. D., Troy P. J., Balch W. M., Adams A. K., Li Y. H. and Mackenzie F. T. (1999) Biologically mediated dissolution of calcium carbonate above the chemical lysocline? *Deep-Sea Res Pt I* **46**, 1653–1669.

Morales L. V., Sigman D. M., Horn M. G. and Robinson R. S. (2013) Cleaning methods for the isotopic determination of diatom-bound nitrogen in non-fossil diatom frustules. *Limnol. Oceanogr. Methods* **11**(2), 101–112.

Morales L. V., Granger J., Chang B. X., Prokopenko M. G., Plessen B., Gradinger R. and Sigman D. M. (2014). Elevated 15N/14N in particulate organic matter, zooplankton, and diatom frustule-bound nitrogen in the ice-covered water column of the Bering Sea eastern shelf. Deep Sea Res. Part II, 109, 100–111. Understanding Ecosystem Processes in the Eastern Bering Sea III.

Movellan A. (2013). La biomasse des foraminifères planctoniques actuels et son impact sur la pompe biologique de carbone. Ph. D. thesis, Sciences de la Terre, Université d'Angers, Français.

Mulitza S., Dürkoop A., Hale W., Wefer G. and Niebler H. S. (1997) Planktonic foraminifera as recorders of past surface-water stratification. *Geology* **25**, 335–338.

Mulitza S., Donner B., Fischer G., Paul A., Pätzold J., Rühlemann C. and Segl M. (2004). The South Atlantic in the late quaternary: reconstruction of material budgets and current systems. Springer, Berlin. Chap. The South Atlantic oxygen isotope record of planktic foraminifera, pages 121–142.

Muscatine L., Goiran C., Land L., Jaubert J., Cuif J. P. and Allemand D. (2005) Stable isotopes ($\delta^{13}C$ and $\delta^{15}N$) of organic matrix from coral skeleton. *Proc. Natl. Acad. Sci. USA* **102**, 1525–1530.

Nydahl F. (1978) On the peroxodisulphate oxidation of total nitrogen in waters to nitrate. *Water Res.* **12**, 1123–1130.

Peeters F., Ivanova E., Conan S., Brummer G.-J., Ganssen G., Troelstra S. and van Hinte J. (1999) A size analysis of planktic foraminifera from the Arabian Sea. *Mar. Micropaleontol.* **36**(1), 31–63.

Pennock J. R., Velinsky D. J., Ludlam J. M., Sharp J. H. and Fogel M. L. (1996) Isotope fractionation of ammonium and nitrate during their uptake by Skeletonema Costatum: implications for the $\delta^{15}N$ dynamics under bloom conditions. *Limnol. Oceanogr.* **41**(3), 451–459.

Popp B. N., Graham B. S., Olson R. J., Hannides C. C. S., Lott M. J., López-Ibarra G. A., Galván-Magaña F. and Fry B. (2007) Insight into the trophic ecology of Yellowfin Tuna, Thunnus albacares, from compound-specific nitrogen isotope analysis of proteinaceous amino acids. *Terrestrial Ecology* **1**, 173–190.

Qi H., Coplen T. B., Geilmann H., Brand W. A. and Böhlke J. K. (2003) Two new organic reference materials for $\delta^{13}C$ and $\delta^{15}N$ measurements and a new value for the $\delta^{13}C$ of NBS 22 oil. *Rapid Commun. Mass Spectrom.* **17**, 2483–2487.

Ravelo A. C. and Fairbanks R. G. (1992) Oxygen isotopic composition of multiple species of planktonic foraminifera: Recorders of the modern photic zone temperature gradient. *Paleoceanography* **7**(6), 815–831.

Ren H., Sigman D. M., Meckler A. N., Plessen B., Robinson R. S., Rosenthal Y. and Haug G. H. (2009) Foraminiferal isotope evidence of reduced nitrogen fixation in the ice age atlantic ocean. *Science* **323**, 244–248.

Ren H., Sigman D. M., Thunell R. C. and Prokopenko M. G. (2012) Nitrogen isotopic composition of planktonic foraminifera from the modern ocean and recent sediments. *Limnol. Oceanogr.* **57**(4), 1011–1024.

Ren H., Studer A. S., Serno S., Sigman D. M., Winckler G., Anderson R. F., Oleynik S., Gersonde R. and Haug G. H. (2015) Glacial-to-interglacial changes in nitrate supply and consumption in the subarctic North Pacific from microfossil-bound N isotopes at two trophic levels. *Paleoceanography* **30**, 1217–1232.

Robbins L. L. and Brew K. (1990) Proteins from the organic matrix of core-top and fossil planktonic foraminifera. *Geochim. Cosmochim. Acta* **54**, 2285–2292.

Robinson R. S., Brunelle B. G. and Sigman D. M. (2004) Revisiting nutrient utilization in the glacial Antarctic: evidence from a new diatom-bound N isotope method. *Paleoceanography* **19**(PA3001), 1–13.

Saino T. and Hattori A. (1980) ^{15}N natural abundance in oceanic suspended particulate matter. *Nature* **283**, 752–754.

Salmon K. H., Anand P., Sexton P. F. and Conte M. (2015) Upper ocean mixing controls the seasonality of planktonic foraminifer fluxes and associated strength of the carbonate pump in the oligotrophic North Atlantic. *Biogeosciences* **12**(1), 223–235.

Schiebel R. (2002) Planktic foraminiferal sedimentation and the marine calcite budget. *Global Biogeochem. Cycles* **16**(4), 1–21.

Schiebel R. and Hemleben C. (2005) Modern planktic Foraminifera. *Paläontologische Zeitschrift* **79**(1), 135–148.

Schiebel R. and Hemleben C. (2017) *Planktic Foraminifers in the Modern Ocean*. Springer-Verlag, Berlin Heidelberg.

Schiebel R., Hiller B. and Hemleben C. (1995) Impacts of storms on Recent planktic foraminiferal test production and $CaCO_3$ flux in the North Atlantic at 47°N, 20°W (JGOFS). *Mar. Micropaleontol.* **26**(1), 115–129.

Schiebel R., Bijma J. and Hemleben C. (1997a) Population dynamics of the planktic foraminifer Globigerina bulloides from the eastern North Atlantic. *Deep-Sea Res. Pt I* **44**, 1701–1713.

Schiebel R., Zeltner A. and Hemleben C. (1997b). Produktion und vertikaler FluX kalkigen Planktons im NE-Atlantik und der Arabischen See. Page 47–48 of: Giese M. and Wefer G. (eds), Bericht über den 5. JGOFS-Workshop. 27/28 November 1996 in Bremen, Berichte aus dem Fachbereich Geowissenschaften Universität Bremen, vol. 89.

Schiebel R., Waniek J., Zeltner A. and Alves M. (2002) Impact of the Azores front on the distribution of planktic foraminifers, shelled gastropods, and coccolithophorids. *Deep-Sea Res. Pt II* **49**, 4035–4050.

Schiebel R., Barker S., Lendt R., Thomas H. and Bollmann J. (2007) Planktic foraminiferal dissolution in the twilight zone. *Deep-Sea Res. Pt II* **54**, 676–686.

Schmuker B. and Schiebel R. (2002) Planktic foraminifers and hydrography of the eastern and northern Caribbean Sea. *Mar. Micropaleontol.* **46**(3–4), 387–403.

Sigman D. M., Altabet M. A., McCorkle D. C., François R. and Fischer G. (1999a) The $\delta^{15}N$ of nitrate in the Southern Ocean: consumption of nitrate in surface waters. *Global Biogeochem. Cycles* **13**(4), 1149–1166.

Sigman D. M., Altabet M. A., François R., McCorkle D. C. and Gaillard J. F. (1999b) The isotopic composition of diatom-bound nitrogen in Southern Ocean sediments. *Paleoceanography* **14**(2), 118–134.

Sigman D. M., Casciotti K. L., Andreani M., Barford C., Galanter M. and Böhlke J. K. (2001) A bacterial method for the nitrogen isotopic analysis of nitrate in seawater and freshwater. *Anal. Chem.* **73**, 4145–4153.

Spero H. J. (1988) Ultrastructural examination of chamber morphogenesis and biomineralization in the planktonic foraminifer *Orbulina universa*. *Mar. Biol.* **99**(1), 9–20.

Spero H.J. (1998). Isotope Paleobiology and Paleoecology. Special publication edn. Paleontological Society Papers, vol. 4. The

Paleontological Society. Chap. Life History and Stable Isotope Geochemistry of Planktonic Foraminifera.

Spero H. J. and Parker S. L. (1985) Photosynthesis in the symbiotic planktonic foraminifer Orbulina universa, and its potential contribution to oceanic primary productivity. *J. Foramin. Res.* **15**(4), 273–281.

Spindler M., Hemleben C., Salomons J. and Smit L. (1984) Feeding behavior of some planktonic foraminifers in laboratory cultures. *J. Foramin. Res.* **14**(4), 237–249.

Stathoplos L. and Hare P.E. (1989). Amino acids in planktonic foraminifera: are they phylogenetically useful? Pages 329–338 of: Crick R.E. (ed), Origin, Evolution, and Modern Aspects of Biomineralization in Plants and Animals. Proc. 5th Intl. Symp. Biomineral. University of Texas, Arlington, Texas: Springer Science & Business Media.

Steinberg D. K., Carlson C. A., Bates N. R., Johnson R. J., Michaels A. F. and Knap A. H. (2001) Overview of the US JGOFS Bermuda Atlantic Time-series Study (BATS): a decade-scale look at ocean biology and biogeochemistry. *Deep-Sea Res. Pt II* **48**, 1405–1447.

Steinhardt J., de Nooijer L. L. J., Brummer G.-J. and Reichart G.-J. (2015) Profiling planktonic foraminiferal crust formation. *Geochem. Geophys. Geosyst.* **16**, 2409–2430.

Straub M., Sigman D. M., Ren H., Martínez-García A., Nele Meckler A. and Haug G. H. (2013) Changes in North Atlantic nitrogen fixation controlled by ocean circulation. *Nature* **501**, 200–204.

Sumper M., Brunner E. and Lehmann G. (2005) Biomineralization in diatoms: characterization of novel polyamines associated with silica. *FEBS Lett.* **579**(17), 3765–3769.

Takahashi K. and Bé A. W. H. (1984) Planktonic foraminifera: factors controlling sinking speeds. *Deep Sea Res.* **31**(12), 1477–1500.

Tolderlund D. S. and Bé A. W. H. (1971) Seasonal distribution of planktonic foraminifera in the Western North Atlantic. *Micropaleontology* **17**(3), 297–329.

Uhle M. E., Macko S. A., Spero H. J., Engel M. H. and Lea D. W. (1997) Sources of carbon and nitrogen in modern planktonic foraminifera: the role of algal symbionts as determined by bulk and compound specific stable isotopic analyses. *Org. Geochem.* **27**(3/4), 103–113.

Uhle M. E., Macko S. A., Spero H. J., Lea D. W., Ruddiman W. F. and Engel M. H. (1999) The fate of nitrogen in the Orbulina universa foraminifera–symbiont system determined by nitrogen isotope analyses of shell-bound organic matter. *Limnol. Oceanogr.* **44**(8), 1968–1977.

Verrado D. J., Froelich P. N. and McIntyre A. (1990) Determination of organic carbon and nitrogen in marine sediments using the Carlo Erba NA-1500 analyzer. *Deep-Sea Res.* **37**, 157–165.

Wada E. and Hattori A. (1978) Nitrogen isotope effects in the assimilation of inorganic nitrogenous compounds by marine diatoms. *Geomicrobiol. J.* **1**(1), 85–101.

Waser N. A. D., Harrison P. J., Nielsen B., Calvert S. E. and Turpin D. H. (1998) Nitrogen isotope fractionation during the uptake and assimilation of nitrate, nitrite, ammonium, and urea by a marine diatom. *Limnol. Oceanogr.* **43**(2), 215–224.

Weigand M. A., Foriel J., Barnett B., Oleynik S. and Sigman D. M. (2016) Updates to instrumentation and protocols for isotopic analysis of nitrate by the denitrifier method. *Rapid Commun. Mass Spectrom.* **30**(12), 1365–1383, RCM-15-0493.R1.

Welch B. L. (1947) The generalization of "Student's" problem when several different population variances are involved. *Biometrika* **34**(1–2), 28–35.

Associate editor: Jack J. Middelburg